UNIVERSITY/INDUSTRY AIRCRAFT ENGINE RELIABILITY CONSORTIUM

ENGINE TITANIUM CONSORTIUM – PHASE 1

FINAL REPORT
94-G-048

PART III

1. Theses abstracts
   - Kim Han, Ph.D. "Relationship Between the Ultrasonic Grain Noise and Microstructure in Two-Phase Microstructures"
   - Paul Panetta, Ph.D., "Backscattering and Attenuation During the Propagation of Ultrasonic Waves in Duplex Titanium Alloys"
   - Prasad, A. N. Shanti, MS, "Multimedia Presentation In A Multicast Communication Environment"
   - Brian Boyd, MS, "Development And Application Of Geometrical Models Of Defects For Ultrasonic Nondestructive Evaluation In Aircraft Engine Alloys"
   - Kit Weng Loo, MS, "An Improved Ultrasonic Data Acquistion System"
   - Kannan Srinivasn, MS, "The Development of an Ultrasonic Flaw Detection Protocol: Signal Acquistion and Processing"
   - S.L. Jeng, MS, "Improved Approximate Confidence Intervals for Censored Data"

Backscattering and Attenuation During the Propagation of
Ultrasonic Waves in Duplex Titanium Alloys

Paul Donald Panetta

Major Professor: R. Bruce Thompson

Iowa State University

This dissertation reports results from studies of the interactions between the microstructure/macrostructure of titanium alloys and propagating ultrasonic waves. Attention is focused on the interactions which cause backscattering and attenuation. Experimental studies will be reported which show that the phase aberration contribution to attenuation does not remove energy from the propagating beam, and a physical picture is developed. A simple ray model which encompasses the ideas presented in the physical picture is used to predict attenuation for propagation in single phase materials with elongated grains. In addition, a general theory for attenuation that includes some degree of multiple scattering is presented that can allow for texture effects and duplex microstructures in its most general form. Numerical predictions from the general attenuation theory and an existing backscattering theory are then compared with experimental measurements of the attenuation and backscattering coefficient in a Ti-6Al-4V specimen that contains elongated macrograins consisting of colonies that are modeled as ellipsoids. Agreement between the experimental and theoretical determination of the backscattering coefficient is extremely good if the effects of texture is included. Agreement with attenuation is favorable.

Relationship Between the Ultrasonic Grain Noise and Microstructure in Two-Phase Microstructures

Yanghyong Kim Han

Major Professor: R. Bruce Thompson

Iowa State University

The relationship between grain noise and microstructure in two-phase materials has been studied. The grain noise is one of important factors which controls the detectability of small flaws in advanced materials. The grain noise is dictated by various microstructures such as alloying elements, crystallographic orientation or texture. However, little research has been done to quantify those effects, especially for the two-phase materials because of complexity. This thesis presents quantitative study of those effects for a model system, Ti-64 (two-phase titanium alloy) based on Independent Scattering Model and General Backscattering Model. Materials such as Ti-64 shows several dimension scales of microstructure (macrograin, colony and crystallite) due to crystallographic orientation relationship between phases. Each microstructure contributes to grain noise uniquely. In low k region, macrograins are dominating. On the other hand, in high k region, colonies are controlling the grain noise.

Development and application of geometrical models of defects for ultrasonic nondestructive evaluation in aircraft engine alloys.

Brian Lee Boyd

Major Professors: R. Bruce Thompson and James Oliver

Iowa State University

This thesis describes the development and application of geometrical models of defects for ultrasonic nondestructive evaluation in aircraft engine alloys. The major part of this work was conducted as part of the efforts of the Engine Titanium Consortium, which currently conducts an extensive study of the ultrasonic response and detectability of a number of naturally occurring hard-alpha defects found in titanium billets. These naturally occurring defects are highly irregular in shape and inhomogeneous in composition, and we would like to assess the extent to which their responses can be predicted by available ultrasonic scattering models. Three dimensional geometrical (surface and solid) models of the hard-alpha defects are needed in order to obtain the geometrical and material properties to drive the ultrasonic model calculations and the subsequent probability-of-detection evaluation. These models are to be derived from metallographic cross-section images taken from destructive sectioning of the defect regions. The reconstruction of defect begins with the boundary determination of the respective defect regions on each of the metallographs by utilizing some image processing algorithms. The three-dimensional geometrical model then follows by using the state-of-the-art non-uniform rational b-spline techniques. Once the geometrical models are constructed, the complete material properties can be interpolated within the volume or on the surface of the defects. In this thesis, detailed procedures of defect reconstruction are discussed and preliminary results are presented. The use of the defect reconstruction as an input to ultrasonic signal modeling will also be illustrated.

2. Publication citations

1. Three volumes of the Open Forum Proceedings have been published documenting all aspects of the ETC Phase I program. Copies were provided to the Technical Monitor.
2. M. F. X. Gigliotti, R. S. Gilmore, and L. C. Perocchi, "Microstructure and Sound Velocity of Ti-N-O Synthetic Inclusions in Ti-6Al-4V", Metallurgical and Materials Transactions A, Vol. 25A, pp. 2321-2329 (1994).
3. F.J. Margetan, K.Y. Han, I. Yalda, Scot Goettsch, and R.B. Thompson, "The practical application of grain noise models in titanium billets and forgings", Rev. of Progress in QNDE, 14B, D.O. Thompson and D.E. Chimenti, eds., (Plenum Press, N.Y., 1995) p. 2129-2136.
4. C.P. Chiou, F.J. Margetan and R.B. Thompson, " Ultrasonic signal characterizations of flat bottom holes in titanium alloys: experiment and theory", Rev. of Progress in QNDE, 14B, D.O. Thompson and D.E. Chimenti, eds., (Plenum Press, N.Y., 1995) p. 2121-2128.
5. I. Yalda, F.J. Margetan, K.Y. Han and R.B. Thompson, "Survey of ultrasonic grain noise characteristics in jet engine titanium", Rev. of Progress in QNDE, 15B, D.O. Thompson and D.E. Chimenti, eds., (Plenum Press, N.Y., 1996) p. 1487-1494.
6. F.J. Margetan, I. Yalda and R.B. Thompson, "Predicting gated-peak grain noise distributions for ultrasonic inspections of metals", Rev. of Progress in QNDE, 15B, D.O. Thompson and D.E. Chimenti, eds., (Plenum Press, N.Y., 1996) p. 1509-1516.
7. P. D. Panetta, F. J. Margetan, I. Yalda and R. B. Thompson, "Ultrasonic Attenuation Measurements in Jet-Engine Titanium Alloys", in Rev. of Progress in QNDE, 15B, eds. D.O. Thompson and D.E. Chimenti (Plenum, New York, 1996), p. 1525.
8. C.P. Chiou, F.J. Margetan and R.B. Thompson, "Modeling of ultrasonic signals from weak inclusions", Rev. of Progress in QNDE, 15A, D.O. Thompson and D.E. Chimenti, eds., (Plenum Press, N.Y., 1996) p. 49-55
9. F.J. Margetan, I. Yalda, R.B. Thompson, J. Umbach, U. Suh, P.J. Howard, D.C. Copley, and R. Gilmore, "Ultrasonic grain noise modeling: recent applications to engine titanium inspections", Rev. of Progress in QNDE, 16B, D.O. Thompson and D.E. Chimenti, eds., (Plenum Press, N.Y., 1997) p. 1555-1562.
10. P. D. Panetta, F. J. Margetan, I. Yalda and R. B. Thompson, "Observation and Interpretation of Microstructurally Induced Fluctuations of Back-Surface Signals and Ultrasonic Attenuation in Titanium Alloys", Rev. of Progress in QNDE, 16B, D.O. Thompson and D.E. Chimenti, eds., (Plenum Press, N.Y., 1997), p. 1547-1554.
11. C.P. Chiou, F.J. Margetan, R.B. Thompson and B. Boyd, "Development of ultrasonic models for hard-alpha inclusions in titanium alloys", Rev. of Progress in QNDE, 16B, D.O. Thompson and D.E. Chimenti, eds., (Plenum Press, N.Y., 1997) p. 1529-1536
12. I. Yalda, P.D. Panetta, F.J. Margetan and R. B. Thompson, "Characterization of ultrasonic focused Transducers using axial scans and C-scans", Rev. of Progress in QNDE, 16, D.O. Thompson and D.E. Chimenti, eds., (Plenum Press, N.Y., 1997) p. 927-934.
13. F.J. Margetan, P.D. Panetta, and R.B. Thompson, "Ultrasonic signal attenuation in engine titanium alloys", in Rev. of Progress in QNDE, 17B, eds. D.O. Thompson and D.E. Chimenti, (Plenum, New York, 1998) p. 1469-1476.
14. R.B. Thompson, F.J. Margetan, I. Yalda, C. P. Chiou and P.D. Panetta, and, "Coupling microstructure outputs of process models to ultrasonic inspectability ", in Rev. of Progress in QNDE, 17B, eds. D.O. Thompson and D.E. Chimenti, (Plenum, New York, 1998) p. 1847-1453.
15. C.P. Chiou, Isaac Yalda, F.J. Margetan, and R.B. Thompson, "The use of ultrasonic flaw and noise models in designing titanium test blocks", Rev. of Progress in QNDE, 17B, D.O. Thompson and D.E. Chimenti, eds., (Plenum Press, N.Y., 1997) p. 2069-2076.
16. P. D. Panetta, R. B. Thompson and F. J. Margetan, "Use of electron backscatter diffraction in understanding texture and the mechanisms of backscattered noise

generation in titanium alloys", in Rev. of Progress in QNDE, 17A, eds. D.O. Thompson and D.E. Chimenti, (Plenum, New York, 1998) p. 89-96.

17. I. Yalda, F.J. Margetan and R.B. Thompson "Use of Rician distributions to predict distributions of ultrasonic flaw signals in the presence of backscattered noise", in Rev. of Progress in QNDE, 17A, eds. D.O. Thompson and D.E. Chimenti, (Plenum, New York, 1998) p. 105-111.
18. A. Minachi, F.J. Margetan and R.B. Thompson "Reconstruction of a piston transducer beam using multi-Gaussian beams (MGB) and its applications", in Rev. of Progress in QNDE, 17A, eds. D.O. Thompson and D.E. Chimenti, (Plenum, New York, 1998) p. 907-914.
19. K.Y. Han and R. B. Thompson, "Relationship Between the Two-Point Correlation of Elastic Constants and Backscattered Noise in Two-Phase Titanium Alloys", Rev. of Progress in QNDE ,Vol. 14, 67-74 (1995).
20. Panetta, P. D. and Thompson, R. B., "Ultrasonic Attenuation and Velocity in Duplex Titanium Alloys," Rev. of Progress in QNDE, 18, edited by D. O. Thompson and D. E. Chimenti, Plenum Press, New York, NY, in press.
21. Panetta, P. D., Thompson, R. B., and Margetan, F. J., "Use of Orientation Imaging Microscopy™ in Understanding Mechanisms of Back-Scattered Noise Generation and Hard-Alpha Inclusion Reflectivity in Titanium Alloys", Rev. of Progress in QNDE, 17, edited by D. O. Thompson and D. E. Chimenti, Plenum Press, New York, NY, in press.
22. Margetan, F. J., Thompson, R. B., and Lerch, T. P., "An Analytical Approximation for a Common Grain Noise Diffraction Integral," Rev. of Progress in QNDE, 18, edited by D. O. Thompson and D. E. Chimenti, Plenum Press, New York, NY, in press.
23. Thompson, R. B., "Use of UT models in titanium inspection development," Rev. of Progress in QNDE, 16B, edited by D. O. Thompson and D. E. Chimenti, pp. 1537-1545, Plenum Press, New York, NY, 1997.
24. Thompson, R. B., "A generalized model of the effects of microstructure on ultrasonic backscattering and flaw detection," Rev. of Progress in QNDE, 15B, edited by D. O. Thompson and D. E. Chimenti, pp. 1471-1477, Plenum Press, New York, NY, 1996.
25. Gray, T. A.: "Application of Measurement Models to Specification of Ultrasonic Inspections," in Rev. of Progress in QNDE, 16, D.O. Thompson and D.E. Chimenti, eds., pp. 2061-2068. (Plenum Press, New York, 1997).
26. Gray, T. A.: "Ultrasonic Inspectability Models for Jet Engine Forgings," to be published in Rev. of Progress in QNDE, 17, D.O. Thompson and D. E. Chimenti, eds., pp.2053-2060. (Plenum Press, New York, 1998).
27. P. Howard, D. Copley, and R. Gilmore, "Transducer design for high sensitivity ultrasonic inspection of titanium," Rev. of Progress in QNDE, 16,A eds. D.O. Thompson and D.E. Chimenti, (Plenum Press, New York, 1997), pp.893-900.
28. J. A. Umbach, R. A. Roberts, "Ultrasonic Phased Array Transducers -Model and Experiment", presented at ASNT conference, Pittsburgh, PA, October, 1997.
29. C.-P. Chiou, R. B. Thompson and L. W. Schmerr, "Model-Based Signal Processing for Ultrasonic Flaw Detection: Simulation Studies," Rev. of Progress in QNDE, D. O. Thompson and D. E. Chimenti eds., 12A, 1993, pp. 703-710.
30. S. Prasad, S. Udpa, L. Udpa and C.-P. Chiou, "Detection of Hard-Alpha Regions in Titanium Using Wavelet Transform Based Techniques," Rev. of Progress in QNDE, D. O. Thompson and D. E. Chimenti eds., 13A, 1994, pp. 801-808.
31. K. Srinivasan, C.-P. Chiou, and R. B. Thompson, "Ultrasonic Flaw Detection Using Signal Matching Techniques," Rev. of Progress in QNDE, D. O. Thompson and D. E. Chimenti eds., 14A, 1995, pp. 711-718.

32. C.-P. Chiou, R. B. Thompson and L. W. Schmerr, "Ultrasonic Signal-to-Noise Enhancement Using Adaptive Filtering Techniques," Rev. of Progress in QNDE, D. O. Thompson and D. E. Chimenti eds., 14A, 1995, pp. 727-732.
33. P. Howard, D. Copley, and R. Gilmore, "The application of a dynamic threshold to c-scan images with variable noise," *Rev. of Progress in QNDE, 17,* eds. D.O. Thompson and D.E. Chimenti, (Plenum Press, New York, 1998).
34. P. Howard, D. Copley, J. Young, E. Nieters, and R. Gilmore, "An improved methodology for the inspection of titanium alloys," *Proceedings of the 1996 IEEE Ultrasonics Symposium, 1*, ed. M. Levy, S. Schneider, and B. McAvoy, (IEEE Press, 1996), pp. 727-730.
35. P. Howard and R. Gilmore, "Ultrasonic noise and the volume of the ultrasonic pulse," *Rev. of Progress in QNDE 15*, eds. D.O. Thompson and D.E. Chimenti, (Plenum Press, New York, 1996), pp. 1495-1502.
36. P. Howard, R. Burkel, and R. Gilmore, "The statistical distribution of grain noise in ultrasonic C-scan images," *Rev. of Progress in QNDE 15*, eds. D.O. Thompson and D.E. Chimenti, (Plenum Press, New York, 1996), pp. 1517-1524.
37. P. Howard, D. Copley, E. Nieters, J. Young, M. Keller, and R. Gilmore, "Ultrasonic inspection of cylindrical titanium billet," *Am. Society of Nondestructive Testing Fall Conference*, 1994.
38. C. Annis, (1997) "Role of Statistical Test Design in Measuring NDE Reliability," European-American Workshop Determination of Reliability and Validation of NDE, 19 June, 1997, Berlin, Germany.
39. R.H. Burkel, D.J. Sturges, W.T. Tucker, and R.S. Gilmore, "Probability of Detection for Applied Ultrasonic Inspections," Review of Progress in QNDE, vol. 15B, eds. D.O. Thompson and D.E. Chimenti, (Plenum Press, New York, 1996), pp. 1991-1998.
40. Thompson, R. B., "Overview of the ETC POD Methodology," Rev. of Progress in QNDE, 18, edited by D. O. Thompson and D. E. Chimenti, Plenum Press, New York, NY, in press.
41. C.-P. Chiou, L. W. Schmerr and R. B. Thompson, "Ultrasonic Flaw Detection Using Neural Network Models and Statistical Analysis: Simulation Studies," Rev. of Progress in QNDE, D. O. Thompson and D. E. Chimenti eds., 12A, 1993, pp. 789-795.
42. C.-P. Chiou, L. W. Schmerr and R. B. Thompson, "Statistical Detection for Ultrasonic NDE," Rev. of Progress in QNDE, D. O. Thompson and D. E. Chimenti eds., 13A, 1994, pp. 871-878.
43. W. Q. Meeker, R. B. Thompson, C.-P. Chiou, S.-L. Jeng and W. T. Tucker, "Methodology for Estimating Nondestructive Evaluation Capability," Rev. of Progress in QNDE, D. O. Thompson and D. E. Chimenti eds., 15B 1996, pp. 1983-1990.
44. W.Q. Meeker, S.-L. Jeng, C.-P. Chiou and R. Bruce Thompson, "Improved Methodology for Predicting POD of Detecting Synthetic Hard-Alpha Inclusions in Titanium," in Rev. of Progress in QNDE, D. O. Thompson and D. E. Chimenti eds., 16B, 1997, pp. 2021-2028.
45. B. Boyd, C.-P. Chiou, R. B. Thompson and J. Oliver, "Development of Geometrical Models of Hard-Alpha Inclusions for Ultrasonic Analysis in Titanium Alloys," in Rev. of Progress in QNDE, D. O. Thompson and D. E. Chimenti eds., 17A, 1998, pp. 823-830.
46. Rough Surface Effects on Incoherent Scattering from Random Volumetric Scatterers: Approximate Analytic Series Solution, M. Bilgen and J. H. Rose, J. Am. Acoust. Soc. **96**, 2856 (1994).
47. Acoustic double-reflection and transmission at a rough water-solid interface, J. H. Rose, M. Bilgen and P. B. Nagy, J. Acoust. Soc. Am. **95**, 3242 (1994).
48. Focused ultrasonic probes and the effects of surface roughness on material noise, M. Bilgen and J. H. Rose, Rev. of Progress in QNDE, **13**, 1769 (1994).

49. Doubly coherent transmission at rough surfaces and its implications for ultrasonic inspection, J.H. Rose, Rev. of Progress in QNDE, **13**, 1753 (1994).
50. "Mean and Variance of the Ultrasonic Signal from a Scatterer Beneath a Rough Surface: Theory", M. Bilgen and J. H. Rose, J. Acoust. Soc. Am. **98**, 2217 (1995).
51. Ultrasonic signals from "worst-case" hard-alpha inclusions beneath a random rough surface, J.H. Rose, Rev. of Progress in QNDE, **14**, 1837 (1995).
52. Excess scattering induced loss at a rough surface due to partially coherent double reflection, J.H. Rose, Rev. of Progress in QNDE, **14**, 1845 (1995).
53. Variance of the ultrasonic signal from a defect beneath a rough surface, J.H. Rose, Rev. of Progress in QNDE, **15**, 1463 (1996).
54. Acoustic Backscatter from materials with rough surfaces and finite microstructures: Theory, M. Bilgen and J.H. Rose, J. Acoust. Soc. Am, **101**, 264 (1997).
55. Acoustic signal-to-noise ratio for flaws beneath a randomly rough surfaces and in the presence of microstructure, M. Bilgen and J.H. Rose, J. Acoust. Soc. Am, **101**, 272 (1997).
56. K. Smith, "Engine Perspectives on Aging Aircraft", presentation at the 41st International Symposium of SAMPE, March 1997.
57. A. D'Orvilliers, and D. Bryson, "Application of the ETC Portable Scanner to Disk Inspection", Proceedings of the Open Forum, November 1997.
58. R. J. Filkins, J. P. Fulton, T. C. Patton, and J. D. Young, "Recent advances and implementations of flexible circuit eddy current technology", Rev. of Progress in QNDE, v. 16, ed. by D. O. Thompson and D.E. Chimenti, Plenum Press, New York, NY, 1997.
59. T. Patton, R. Filkins, J. Fulton, K. Hedengren, J. Young, C. Granger, and T. Hewton, "Development of a hand-held, flexible eddy current probe for inspection of curving surfaces", Rev. of Progress in QNDE, v. 15, ed. by D. O. Thompson and D. E. Chimenti, Plenum Press, New York, NY, 1996.
60. J. P. Fulton, K. Hedengren, J. Young, T. Patton, R. Filkins, "Optimizing the design of flexible multilayer eddy current probes - A theoretical and experimental study", Rev. of Progress in QNDE, v. 15, ed. by D. O. Thompson and D. E. Chimenti, Plenum Press, New York, NY, 1996.
61. K. Hedengren, J. Fulton, J. Young, T. Patton, R. Filkins and R. Hewes, "Progress in flexible eddy current array technology", Rev. of Progress in QNDE, v. 15, ed. by D. O. Thompson and D. E. Chimenti, Plenum Press, New York, NY, 1996.
62. R. J. Filkins, J. P. Fulton, T. C. Patton, and J. D. Young, "Recent advances and implementations of flexible circuit eddy current technology", Rev. of Progress in QNDE, v. 16, ed. by D. O. Thompson and D.E. Chimenti, Plenum Press, New York, NY, 1997.
63. T. Patton, R. Filkins, J. Fulton, K. Hedengren, J. Young, C. Granger, and T. Hewton, "Development of a hand-held, flexible eddy current probe for inspection of curving surfaces", Rev. of Progress in QNDE, v. 15, ed. by D. O. Thompson and D. E. Chimenti, Plenum Press, New York, NY, 1996.
64. J. P. Fulton, K. Hedengren, J. Young, T. Patton, R. Filkins, "Optimizing the design of flexible multilayer eddy current probes - A theoretical and experimental study", Rev. of Progress in QNDE, v. 15, ed. by D. O. Thompson and D. E. Chimenti, Plenum Press, New York, NY, 1996.
65. K. Hedengren, J. Fulton, J. Young, T. Patton, R. Filkins and R. Hewes, "Progress in flexible eddy current array technology", Rev. of Progress in QNDE, v. 15, ed. by D. O. Thompson and D. E. Chimenti, Plenum Press, New York, NY, 1996.
66. Jay M. Amos, Joseph C. Chao, 'Optimization of a Wide-Field Eddy Current Probe using a Boundary Element Method based Model', Rev. of Progress in QNDE, p. 275, Vol 17, 7/97.

67. Jay M. Amos, Joseph C. Chao, 'Assessment of Eddy Current Inspection Development through Numerical Simulation', American Society of Nondestructive Testing Fall Conference, 10/97.

68. J.M. Amos, D.A. Raulerson, J.C. Chao, N. Nakagawa, 'Model-based Eddy Current Probe Optimization & Processing Methods for Engine Inspections', ATA Open Forum, 11/97

69. N. Nakagawa, J. Chao, and A.N.S. Prasad, "In-service eddy current inspection and computer simulation," in *Nondestructive Testing of Materials*, eds. R. Collins, W.D. Dover, J.R. Bowler, and K. Miya, IOS Press, Amsterdam, 1995.

70. J. C. Chao, N. Nakagawa, D. Raulerson, and J. C. Moulder, "Boundary element method based probe design model validation," in Rev. of Progress in QNDE, 16, pp. 967-972, eds. D. O. Thompson and D. E. Chimenti, Plenum Press, New York, 1997..

71. L. Brasche & K. Smith, "Engine Titanium Consortium: Status of the Contaminated Billet Study", Materials and Process Affordability Keys to the Future, SAMPE 43, p. 1458, June 1998.

3. Scientific Collaborators at Iowa State University

Name	Title
Lisa Brasche	Scientist
Bruce Thompson	Distinguished Professor – AEEM
Bill Meeker	Distinguished Professor - Statistics
Tim Gray	Scientist
Frank Margetan	Associate Scientist
Ron Roberts	Scientist
Thomas Chiou	Assistant Scientist
Jim Rose	Scientist
Norio Nakagawa	Associate Scientist
M. Bilgen	Post Doctoral Fellow
Joe Chao	Post Doctoral Fellow
Ali Minachi	Post Doctoral Fellow
Issac Yalda	Post Doctoral Fellow
Kim Han	Graduate Student
Paul Panetta	Graduate Student
Brian Boyd	Graduate Student
S. Prasad	Graduate Student
K. Loo	Graduate Student
K. Srinivasan	Graduate Student
S.L. Jeng	Graduate Student
Seth Meyer	Undergraduate Student
Scot Goettsch	Undergraduate Student

4. Briefly describe any inventions which resulted from the project and the status of pending patent applications, if any.

None.

5. Provide a technical summary of the activities and results. The information supplied in proposals for further support, updated as necessary, may be used to fulfill this requirement.

Products summary provided on following pages.

6. Include any additional material, either specifically required in the award instrument (e.g. special technical reports or products such as films, books, studies) or which are considered to be useful to the Foundation.

Several technical reports have been submitted to the technical monitor. Those include the following:

- "Summary of Titanium Fundamental Studies of the Engine Titanium Consortium"
- "Inservice Inspection: Development of Portable Eddy Current Inspection Tools for Engine Overhaul Applications"
- "A Methodology For Reliability Assessment For Subsurface Flaws In Engine Components"

Engine Titanium Consortium

Products Summary

Major Products	References[i]
FUNDAMENTAL STUDIES	
Various FBH, synthetic hard alpha, and noise blocks for fundamental studies measurements.	See Appendix A.
Documentation of synthetic hard alpha process	[ii]
Cracks through a peened surface	Unpublished summary report provided in Appendix B
Fundamental property measurements of ultrasonic velocity, backscatter noise, and attenuation for Ti6-4 and Ti-17 from various billet and forging configurations.	[iii] [iv] [v] [vi] [vii] [viii] [ix] [x] [xi] [xii] [xiii] [xiv] [xv] [xvi] [xvii] [xviii] [xix] [xx] [xxi] [xxii] Final Report provided, "Summary of Titanium Fundamental Studies of the Engine Titanium Consortium"
Reports of the literature survey, including citations.	Unpublished summary report provided in Appendix C
PRODUCTION INSPECTION	
UT models including transducer design, hard alpha signal models, and noise models.	[xxiii] [xxiv] [xxv] [xxvi]
Demonstration of optimum (fixed focus) transducers for Ti alloys including characterization on flat plate samples and cylindrical samples.	[xxvii]
Demonstration of ultrasonic phased array hardware for optimal inspection approach in a production environment. [Report on array transducers.]	[xxviii]
Development, implementation, and evaluation of SSP Saft, and alternative signal processing techniques for ultrasonic billet inspection. [1. Algorithms developed under this task. 2. Report of optimized image and signal processing approaches for improved defect detection capability. 3.Report on evaluation of applicability to factory inspection situation.]	[xxix] [xxx] [xxxi] [xxxii]
Demonstration of UT inspection system to achieve the highest practical FBH sensitivity with a goal of 1/64 FBH.	[xxxiii] [xxxiv] [xxxv] [xxxvi] [xxxvii]
Billet inspection specifications	SAE AMS 2628
PROBABILITY OF DETECTION	
POD workshop to determine approach	White paper submitted to FAA.
Catalog of existing data to use as baseline including previous finds and data afforded by program.]	[xxxviii] [xxxix]
Improved statistical methods relating detectability to SNR and flaw characteristics.	[xl] [xli] [xlii] [xliii] Final report to be published entitled, "A Methodology For Reliability Assessment For Subsurface Flaws In Engine Components
Validation of methodology using FBH and SHA samples.	[xliv] [xlv] Final report to be published entitled, "A Methodology For Reliability Assessment For Subsurface Flaws In Engine Components"
Report on the determination of the effects of roughness on POD as a function of physical parameters of the measurement system.	[xlvi] [xlvii] [xlviii] [xlix] [l] [li] [lii] [liii] [liv] [lv] Final report to be published entitled, "A Methodology For Reliability Assessment For Subsurface Flaws In Engine Components"
INSERVICE INSPECTION	
Survey of airlines and consortium members to establish needs for inservice tools	Results included in final report.
Scanning tool which permits EC on bores and webs in drum rotors including delivery of one scanner and demonstration with airline.	[lvi] [lvii] [lviii] [lix] [lx] [lxi] Final report to be published which includes details of scanner and betasite tests, entitled, 'Inservice Inspection: Development of Portable Eddy Current Inspection Tools for Engine Overhaul

Major Products	References[i]
	Applications"
Data acquisition and analysis system to improve the sensitivity and efficiency of NDE techniques which integrates with other inspection tools and commercially available instruments. Includes development of one prototype system and betasite testing	Final report to be published which includes details of scanner and integration of data acquisition, entitled, 'Inservice Inspection: Development of Portable Eddy Current Inspection Tools for Engine Overhaul Applications"
Mechanical device to provide controlled rotation of the low-pressure rotor including fabrication of a prototype rotator, test and 2nd generation refinements.	
Investigation of the use of array probes including identification of potential target applications.	[lxii] [lxiii] [lxiv] [lxv]
2D and 3D image processing algorithms to improve characterization and detection of NDE defect responses to include demonstration of 2D imaging routines for implementation on Data Acquisition/Analysis System (DAS	Final report to be published which includes details of scanner and integration of image processing tools, entitled, 'Inservice Inspection: Development of Portable Eddy Current Inspection Tools for Engine Overhaul Applications"
Demonstration of signal/image processing algorithms for improved sensitivity in galled areas and welds, and near edges	Final report to be published which includes details of scanner and signal processing routines, entitled, 'Inservice Inspection: Development of Portable Eddy Current Inspection Tools for Engine Overhaul Applications"
Design and sensitivity data for novel EC probes.	[lxvi] [lxvii] [lxviii] [lxix]
Electromagnetic field model using BEM capability. Techniques to determine electromagnetic field characteristics for conventional EC element designs including application to new probe designs.	[lxx] [lxxi] [lxxii] [lxxiii] [lxxiv]
CONTAMINATED BILLET STUDY	
Ultrasonic field inspection data for both conventional and the zoned inspection approaches under development by ETC. UT results in formats suitable for disposition of indications and quantitative assessments by POD studies.	Results will be summarized in final CBS report of ETC Phase II Program.
Basic knowledge to improve the detection of hard alpha by developing an understanding of the acoustic, physical and chemical properties of hard alpha	[lxxv] Results will be summarized in final CBS report of ETC Phase II Program.
Evaluation of nonrejectable indications and indication-free portions of the contaminated heat to determine the occurrence of potential ultrasonic misses. To assess the detectability of hard alpha defects at the billet stage including the effects of microstructure (noise banding) and billet surface condition	Results will be summarized in final CBS report of ETC Phase II Program.

Appendix A: List of samples generated by the ETC Phase I program.

Samples	Comments	Sample ID
2 Ti 17 7" diameter billet specimens	Completed	None
Samples of nitrogen stabilized hard alpha "seeds" at each concentration, including no contamination.	Completed	N/A
1 Ti 6-4 block with 8 each #2, #3, #4, and #5 FBH size of cylindrical hard alpha inclusions of 1.6% nitrogen concentration at 1" and 2" depth, longitudinal.	Completed	S940119-1.6N
1 Ti 6-4 block with 8 each #2, #3, #4, and #5 FBH size of cylindrical hard alpha inclusions of 2.6% nitrogen concentration at 1" and 2" depth, longitudinal.	Completed	S940128-2.6N
1 Ti 6-4 block with 8 each #2, #3, #4, and #5 FBH size of cylindrical hard alpha inclusions of 5.9% nitrogen concentration at 1" and 2" depth, longitudinal.	Completed	S940217-5.9N
3 Ti 6-4 forging blocks (6"x6"x6") representative of actual noise levels	Completed	940106NA, NB & NC
2 Ti 6-4 9.5" diameter billet blocks (3"x3"x3") from center section	Completed	022594-2 & -4
2 Ti 6-4 9.5" diameter billet blocks (3"x3"x3") from OD section	Completed	022594-1 & -3
1 Ti 17 7" diameter billet block (3"x3"x3") from center section	Completed	052094-3
2 Ti 17 7" diameter billet block (3"x3"x3") from OD section	Completed	052094-1 & -2
3 Ti 6-4 disk forging blocks (3"x3"x3") from different zones of the forging	Completed	060394-1, -2 & -3
1 Ti 6-4 block with 8 each #1, #2, #3 and #4 FBH @ 1" depth, longitudinal.	Completed	F931213-1.5L
1 Ti 6-4 block with 8 each #1, #2, #3 and #4 FBH @2" depth, longitudinal.	Completed	F931213-2.5L
1 Ti 6-4 block with 8 each #1, #2, #3 and #4 FBH @1" depth, shear.	Completed	F931213-1.5S
1 Ti 6-4 block with 8 each #1, #2, #3 and #4 FBH @2" depth, shear.	Completed	F931213-2.5S
18 specimens of galling on titanium with EDM notches, active area of sample is 1/4" x 1 1/2".	Completed; area constraints limited to 6 EDM notches.	JT8D-LPC1-1
2 aluminum block specimens; machine laser holes in center.	Completed	Al #1,2
2 titanium block specimens; machine laser holes in center.	Completed; added EDM notch specimens 2 Ti, 2 Ni, each containing 15 slots.	Ni #2,3, Ti #1,2
24 Ti complex geometry specimens; machine excimer laser notches (edge of disk lugs)	Disk blade slots containing	817401 – F773743

Samples	Comments	Sample ID
	18 EDM notches	
1 Ti 6-4 block with 8 each #2, #3, #4 and #5 FBH size of cylindrical hard alpha inclusions of 1.5% nitrogen concentration at 1" and 2" depth, shear.	Completed	SA940513-1.5N
1 Ti 6-4 block with 8 each #2, #3, #4 and #5 FBH size of cylindrical hard alpha inclusions of 3.0% nitrogen concentration at 1" and 2" depth, shear.	Completed	SA940513-2.8N
1 Ti 6-4 block with 8 each #2, #3, #4 and #5 FBH size of cylindrical hard alpha inclusions of 6.0% nitrogen concentration at 1" and 2" depth, shear.	Completed	SA940513-5.2N
Ti 6-4 enlarged grain block.	Completed	
1 Ti 6-4 block with 8 each #2, #3, #4 and #5 FBH size of spherical hard alpha inclusions of 1.5% nitrogen concentration at 1" and 2" depth.	Item replaced with block with single size spherical hard alpha inclusions. Various size spheres not feasible due to fabrication constraints.	N/A
1 Ti 6-4 block with 8 each #2, #3, #4 and #5 FBH size of spherical hard alpha inclusions of 3.0% nitrogen concentration at 1" and 2" depth.	Item replaced with block with single size spherical hard alpha inclusions. Various size spheres not feasible due to fabrication constraints.	N/A
1 Ti 6-4 block with 8 each #2, #3, #4 and #5 FBH size of spherical hard alpha inclusions of 6.0% nitrogen concentration at 1" and 2" depth.	Item replaced with block with single size spherical hard alpha inclusions. Various size spheres not feasible due to fabrication constraints.	N/A
1 Ti 17 block with 8 each #1, #2, #3 and #4 FBH @ 1" depth, longitudinal.	Completed	F950508-1.5L
1 Ti 17 block with 8 each #1, #2, #3 and #4 FBH @ 2 "depth, longitudinal.	Completed	F950508-2.5L
1 Ti 17 block with 8 each #1, #2, #3 and #4 FBH @ 1" depth, shear.	Completed	F950508-1.5S
1 Ti 17 block with 8 each #1, #2, #3 and #4 FBH @ 2" depth, shear.	Completed	F950508-2.5S
1 set of 5 "chord" blocks of Ti 6-4 7.0" diameter billet containing 5 each #1 FBH @ metal travel depths of 0.5", 1.2", 2.0", 2.8" and 3.5".	Completed	Heat # 954247B1A

Samples	Comments	Sample ID
1 set of 5 "chord" blocks of Ti 17 7.0" diameter billet containing 5 each #1 FBH @ metal travel depths of 0.5", 1.2", 2.0", 2.8" and 3.5".	Completed	Heat # 973784T2A2
1 set of 8 "chord" blocks of Ti 17 10.0" diameter billet containing 5 each #1 FBH @ metal travel depths of 0.5", 1.35", 2.25", 3.15", 4.05", 4.5", 4.95" and 5.5".	Completed	Heat # 954447
1 set of 8 "chord" blocks of Ti 17 13.0" diameter billet containing 5 each #2 FBH @ metal travel depths of 0.5", 1.5", 2.5", 3.5", 4.5", 5.5", 6.5" and 7.0".	Completed	Heat # 963304B2
1 set of 8 "chord" blocks of Ti 6-4 13.0" diameter billet containing 5 each #2 FBH @ metal travel depths of 0.5", 1.5", 2.5", 3.5", 4.5", 5.5", 6.5" and 7.0".		
20 excimer laser notches in Ti weld specimens; EB w/ flash.	Completed	
Drill 6 FBH in 1 Ti 6-4 9.5" diameter billet block (3"x3"x3") from center section.	Completed	
Drill 6 FBH in 1 Ti 6-4 9.5" diameter billet block (3"x3"x3") from OD section.	Completed	
Drill 6 FBH in 1 Ti 17 7" diameter billet block (3"x3"x3") from OD section.	Completed	
5 specimens for LCF from subsurface defects through peened surface.	Completed	LCF-1, -2, -3 & -4
1 Ti 6-4 bar, 1" or 2" diameter, with a 0.032" diameter by 0.016" thick (ellipsoid) defect of approximately 15% impedance mismatch at 30 degrees tilted from normal.	Completed	
1 Ti 6-4 block, 4"x4"x1", with a 0.032" diameter by 0.016" thick (ellipsoid) defect of approximately 15% impedance mismatch at 30 degrees tilted from normal.	Completed	
1 Ti 17 block with 8 each #2, #3, #4 and #5 FBH size of cylindrical hard alpha inclusions of 1.5% nitrogen concentration at 1" and 2" depth, longitudinal.	Completed	S950316-1.5N
1 Ti 17 block with 8 each #2, #3, #4 and #5 FBH size of cylindrical hard alpha inclusions of 3.0% nitrogen concentration at 1" and 2" depth, longitudinal.	Completed	S941202-2.8N
1 Ti 17 block with 8 each #2, #3, #4 and #5 FBH size of cylindrical hard alpha inclusions of 6.0% nitrogen concentration at 1" and 2" depth, longitudinal.	Completed	S950320-5.2N
1 Ti 17 block with 8 each #2, #3, #4 and #5 FBH size of cylindrical hard alpha inclusions of 1.5% nitrogen concentration at 1" and 2" depth, shear.	Completed	SA950321-1.5N
1 Ti 17 block with 8 each #2, #3, #4 and #5 FBH size of cylindrical hard alpha inclusions of 3.0% nitrogen concentration at 1" and 2" depth, shear.	Completed	SA941201-2.8N
1 Ti 17 block with 8 each #2, #3, #4 and #5 FBH size of cylindrical hard alpha inclusions of 6.0% nitrogen concentration at 1" and 2" depth, shear.	Completed	SA950317-5.2N
1 Ti 17 block with 8 each #2, #3, #4 and #5 FBH size of spherical hard alpha inclusions	Items not delivered due to	N/A

Samples	Comments	Sample ID
of 1.5% nitrogen concentration at 1" and 2" depth, longitudinal.	fabrication constraints	
1 Ti 17 block with 8 each #2, #3, #4 and #5 FBH size of spherical hard alpha inclusions of 3.0% nitrogen concentration at 1" and 2" depth, longitudinal.	Items not delivered due to fabrication constraints	N/A
1 Ti 17 block with 8 each #2, #3, #4 and #5 FBH size of spherical hard alpha inclusions of 6.0% nitrogen concentration at 1" and 2" depth, longitudinal.	Items not delivered due to fabrication constraints	N/A
1 Ti 6-4 block with random synthetic hard alpha defects. The variables that will be random are location within the three dimensions, size of reflector, nitrogen content and the angle of the defect relative to the inspection entry surface.	Completed.	RDB

Crack Propagation Through Peened Surface:

Effects on Detectability

Prepared by Bill Leach, GEAE, Cincinnati, Ohio

A subtask of the ETC Phase I Fundamental Studies intended to investigate the effects of the detectability of a crack propagating through a peened surface. The plan was to use a subsurface hard alpha as the crack initiation site to more nearly simulate what may happen with a true melt related defect in a rotating disk. Unfortunately the specimen preparation resulted in unexplained failure of the HIP joint rather than cracking at the hard alpha. New specimens were not fabricated due to timing and funding issues as well as questionable understanding of what in the preparation led to separation at the weld surface.

Background:

Surface cracks have typically been fabricated by machining a notch into the surface of a specimen. The specimen is then cycled until a crack is initiated from the notch. After the crack is of sufficient size the surface is machined to remove the notch. If intended, the specimen surface is then peened. The specimen is further cyclically loaded to grow the crack to the desired size. This is the process typically used in the fabrication of samples for surface crack POD studies, such as for FPI or eddy current. This process is useful in measuring changes in the strength of an eddy current signal and the background noise that occurs with peening. However, there are a number of unanswered questions, which the subtask would assist in resolving. The questions include:

1. Does a compressive layer below the peened surface force a change in the aspect ratio of a subsurface initiated crack?

2. What is the ultrasonic and eddy current detectability of the cracks below the compressive layer?

3. What is the detectability with ultrasonics, eddy current and fluorescent penetrant inspection when the crack has propagated to the surface? For example, does the compressive layer pinch the crack to hamper FPI?

Ability to place known synthetic hard alpha defects in titanium offered the potential to position a subsurface initiation site at various depths below the surface.

Specimen Fabrication:

Figure 1 shows the design of the blocks. Six defects were included in each specimen. 0.25 inch diameter holes were drilled on 0.5 inch centers in the center section of the block which became the gage section of the fatigue specimen. The holes were drilled 0.5 inch deep into the 0.75 inch thick block. The Ti 6-4 material was machined oversized to allow for machining for the axial fatigue test, see Figure 2, with the defects at desired depths.

Synthetic hard alpha defects were machined from "ingots" of 2.8% N into approximate right cylinders 0.05 inch diameter x 0.05 inch length. Plugs of Ti 6-4 were machined to fill the 0.25 inch holes in the block and had a flat bottom hole in one end to accept a hard alpha seed. This approach was chosen to most easily place the hard alpha well into the block. Rather than attempt to drill a 0.05 inch diameter hole any great depth, the plug provided a convenient method. After fabrication of the first block, a detail was changed. The plugs were chosen from areas of the forging that would provide nearly the same structure size and orientation as the surrounding material. This was necessary to reduce the ultrasonic noise from a drastically different or misaligned structure at the HIP interface.

The plugs with the hard alpha were positioned in the large holes and tack welded. The blocks were then HIP processed to bond the hard alpha to the block and to the plug as well as have the plug bond to the block. The blocks were in turn machined to the fatigue specimen geometry. The distance of the hard alpha defects from the surface that was not machined was measured ultrasonically to provide the dimensions for machining the defects at the

proper depth for the test. The first block was machined such that the hard alpha would be at the surface. The second block was machined to place the hard alpha at approximately 0.008 to 0.011 inch below the surface, i.e. just below the compressive layer of the peened surface. After the first block was machined to the fatigue specimen shape it was peened. Inspections with FPI, EC and UT showed signals from the exposed hard alpha seed.

Experiment:

The first specimen was loaded at 75 ksi and viewed visually at frequent increments with the expectation that the hard alpha seeds would serve as the stress riser and fracture very quickly. There was no indication of any change until 2108 cycles when one of the plugs separated. This was confirmed with eddy current and FPI. Fortunately the failed plug was at the one end of the string of six inserts. A decision was made to change to a four point bending across the three defects at the opposite end of the row of 6 defects. The four point bending load was applied at 75 ksi for 37,000 cycles until cracking was detected around portions of the plugs of the first and third hole and small cracking from the hard alpha into the titanium. These cracks were verified with eddy current and with FPI.

Evaluation:

The destructive evaluation of the first block revealed a few interesting points. First, as mentioned earlier, the ultrasonic inspection of the block to interrogate the HIP joint showed a reflection from the bottom of the plug. The sectioning of the specimen showed that the grain structure had different orientation between the plug and the surrounding titanium. That different structure could easily explain the low-level reflections at the base of the plug after HIP. The solution was to make sure the other blocks had plugs prepared from material very close to the location where the blocks were cut.

The section through the separated plug joints did not lead to any obvious cause. There was no evidence of contamination on the joint surfaces. No conclusion was drawn as to the cause of the separation.

A third observation was important. The hard alpha seeds were severely cracked in all directions, apparently the result of the peening process. This explained the porosity around all six seeds as revealed by FPI of the specimen after peening. This was also thought to possibly explain why the hard alpha seeds did not react as expected when the stress was applied to the specimen. The fractured hard alpha seed reacted much like a hole, i.e. a stress relief rather than stress riser.

This led to the decision to machine the second block such that the hard alpha seeds were just below the peened compressive layer, approximately 0.008 to 0.011 inches. Placing the hard alpha seeds below the surface would protect them from fracturing and preserve the stress riser aspect, however, near a compressive force.

The fatigue specimen was cycled and again failed at the plug interface to the specimen. The destructive evaluations confirmed the separation at the plug interface. There was cracking in the hard alpha in the proper direction relative to the stress and several of these cracks in the seeds had begun to propagate into the surrounding titanium of the plug. The extent of the cracks was limited to approximately 0.003". The hardness of the titanium in the specimen and in the plugs was evaluated with Knoop Hardness and shown to have no significant difference.

Conclusion:

The subtask objectives of determining the effects on NDE detectability caused by crack propagation through a peened surface were not met. Failure of the HIP bond joint between the plug and the surrounding titanium prevented the full stress levels from being applied to the seeds. In addition, the peening of exposed hard alpha seeds fractured the seeds so extensively that they did not serve as risers to the applied stress.

The results and the unused blocks were shared with the TRMD Project funded by the FAA at the Southwest Research Institute.

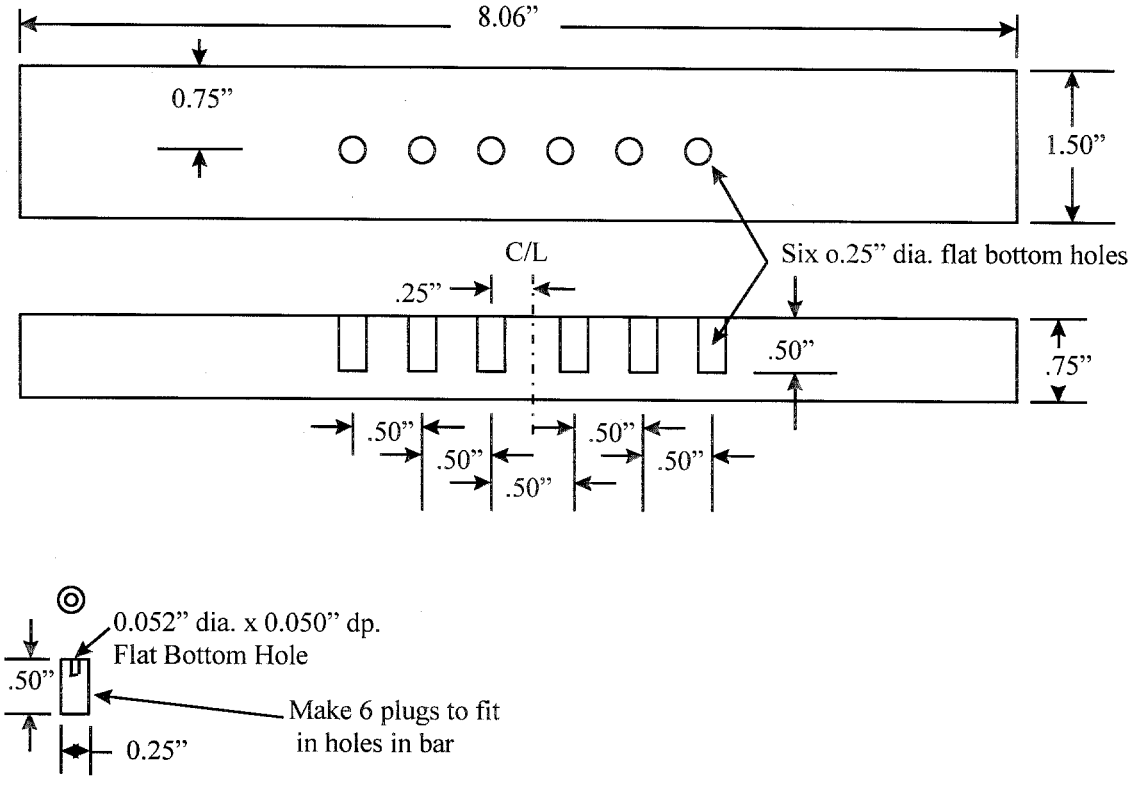

Figure #1

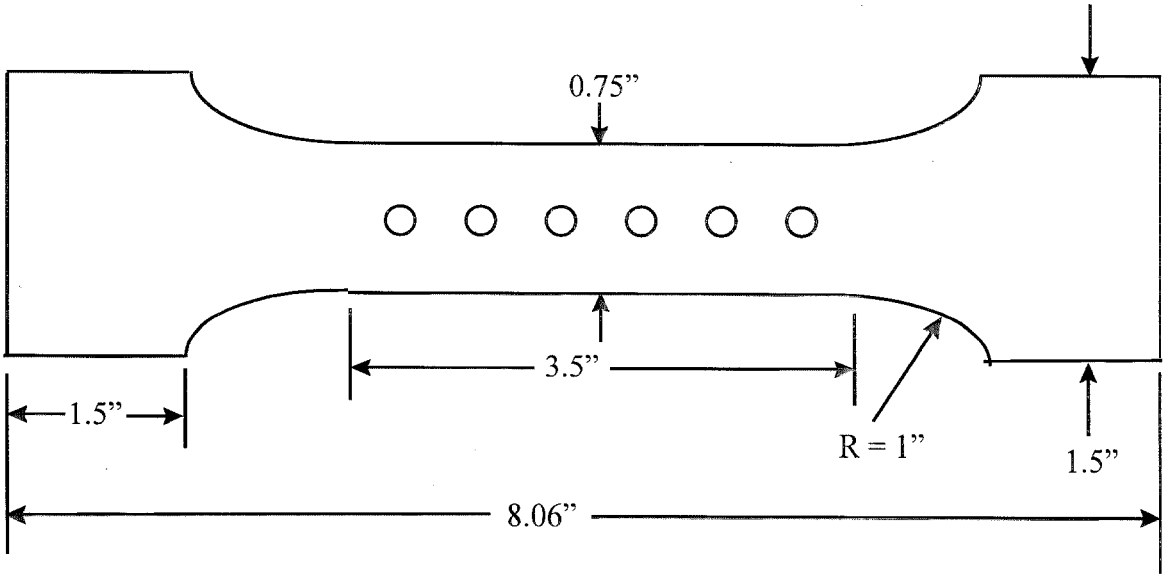

Figure #2

A Review of the Origin and Character of Ingot Defects That May Occur in Aerospace Titanium Alloys and NDE Methods for Detection

James A. Hall, Janet Wade, Lloyd Schaefer, Andy Kinney
Materials and Process Engineering
and
Valerie Peters
Component Investigation
AlliedSignal Engines
20 June 1997

1. ABSTRACT

In support of the Federal Aviation Administration's (FAA) Engine Titanium Consortium (ETC), this paper discusses the origin and characteristics of titanium melt related defects, provides a brief synopsis of experiments conducted to date relating to the evaluation and/or control of melt related defects, the potential nondestructive evaluation (NDE) methods for detecting such defects, and contains literature search references pertaining to these subjects. The report is divided into three sections:
Section 1 of this report contains discussions of Type I defects, high-density inclusions, Type II defects, ingot porosity, and alloy segregation with their definitions, causes and characteristics. Brief synopses of several published experiments relating to sources of nitride inclusions, defect removal, nitride seed development, effect of defects on fatigue properties, and alpha segregation are also included. Forging or conversion related defects are not included in this report.
Section 2 addresses surface and volumetric NDE methods appropriate for detecting and characterizing titanium melt related defects. Image and signal analysis techniques for these methods are identified and discussed as well as various means of measuring NDE methods probability of detection (POD).
Section 3 comments on the utility of the literature review and recommendations for future work.
The references cited in this report are contained in the literature database created as a part of the ETC. The numbers refer to the record number in the database that uses the PROCITE bibliographic software.

2. ACKNOWLEDGMENT

This material is based upon work performed as a part of the Engine Titanium Consortium operated by Iowa State University for the FAA New England Engine and Propeller Directorate and the FAA Technical Center under Grant Number 94-G-048.

3. INTRODUCTION

As a part of the Fundamental Studies in Titanium Task of the ETC, a literature review was undertaken. The literature review had the following purposes:

- Provide the latest information about the formation of various defect types
- Detail any known preventative measures for these types of defects
- Provide information the effect of microstructure and macrostructure of the parent material on detectability
- Catalog data on the material properties
- Provide background information on NDE methods developed by other researchers appropriate to titanium inspection

The intent is to provide data for the formulation of approaches to the various defect detection problems in various material forms. The available literature was reviewed from the NERAC and NOTICE databases. Additional information was also gathered from other available sources such as the following: non-proprietary information solicited from members of the ETC, various domestic producers of titanium, and the Jet Engine Titanium Quality Committee; QNDE proceedings; and other open literature journals.
The synopses provided below are only a sampling and should not be interpreted as being complete, nor inclusive of all key work. The literature database includes other citations of interest for specific issues. These citations may be identified by searching on the desired keywords such as: defects, HDI, inclusions, fatigue life, etc.

4. INGOT DEFECTS, DEFINITION, ORIGINS and CHARACTERISTICS

4.1 TYPE I DEFECTS [1,2,3,4,5]

Type I defects are also known as high interstitial defects (HID), interstitial rich inclusions or low density inclusions (LDI). They are recognized as alpha rich particles interstitially stabilized with nitrogen, oxygen or carbon, or some combinations of these. Their metal alloy content may range from very nearly all titanium to nominal alloy content of the host heat or even of a different alloy.

The embryo form of these defects have a much higher melting point than titanium or Ti alloys and must be consumed by dissolution into the melt. Depending on the relative size and densities of Type I defects, large heavy defects may survive multiple vacuum arc remelt (VAR) processing and smaller lighter defects may survive cold hearth melting (CHM). The defects are substantially harder than the surrounding matrix and may impair fatigue resistance and ductility. The defects are difficult to detect unless associated with voids from mechanical working. The term LDI arose from this void association, however, the alpha-rich phase itself is not of "low density". Of course, creation of a defect during melting as described below will negate some, or all, of the dissolution opportunities offered by melting.

4.2 Sources of Type I defects:

4.2.1 Burned sponge, reactor vessel burning [2, 5]:

Type I defects, originating from this source are attributed to the entry of air into the reaction vessel or vacuum distillation chamber during sponge production. If in a confined volume, air reacts with the titanium sponge, which consumes oxygen (O_2) first, and then the nitrogen (N_2). Nitrogen rich defects resist dissolution in the liquid titanium.

Visual Appearance: Regions of high nitrogen content titanium, when removed from the reactor vessel appear much like the titanium metal, only much more friable. It seldom is golden in color as the near stoichiometric TiN intermetallic would be and therefore not visually separable.

Metallurgical Characteristics: the metallic alloy content will be considerably less than that of the host alloy and the hardness will be significantly higher. Voids may be associated with the larger variety of these defects.

Location in Ingot: Large defects are heavier than the liquid and will tend to concentrate in the bottom 1/3 of the ingot. Smaller (if not dissolved) defects, may be more uniformly distributed. Defects in this family reflect an out-of-control process and may appear in all heats incorporating the culprit sponge lot, and have a size distribution only slightly different than that of the sponge, reduced slightly in size by melting dissolution.

4.2.2 Burned sponge, other [5]:

Type I defects are attributed to burned sponge caused by the following:

- Fires or flashing which may occur during extraction of sponge from the reactor or vacuum distillation chamber
- Downstream processes, such as crushing the chip to sponge
- Drying, in the case of leached sponge
- Sponge may experience combustion during blending and compacting of the electrode

Visual Appearance: In most cases the burned sponge is discolored and visually separable. The refractory particle is brittle and easily crushed. As these causes will affect entire lots of sponge production, a visual examination of selected samples of each lot is often used as a quality control process and finding of HID embryos will disqualify the entire lot from rotor grade applications. However this inspection is ineffective in screening out down stream defect sources from events, such as combustion during the blending operation.

4.2.3 Burned bulk scrap [5]

- Torch cutting. Type I defects may be attributed to torch cutting in preparation of bulk scrap for fabrication. Part of the process detail involves combustion of titanium and in the tight confines of the cutting zone, nitrogen combustion is possible. Furthermore, residual organic material may contribute to carbon stabilization in this region.
- Infoliated ends of mill scrap may contain high O_2 or N_2 levels and should be avoided as they are not easily cleaned.

Metallurgical characteristics: The defect will have normal metallic alloy content of the scrap source. It is unlikely to have cracks or voids unless associated with conversion or forging operations. It may be quite large with an irregular shape.

4.2.4 Burned chips and turnings [5]:

Burned chips and turnings may be another source of HID formers. If burned in a restricted volume, they may become highly contaminated with nitrogen (or carbon in the case of machining chips burned during the machining

operation itself), therefore they are refractory. The shape and size of chip (high surface to volume ratio) leads to rapid dissolution during melting and are unlikely to be serious HID sources in multiple melted ingot, e.g., double or triple VAR, fabricated from electrodes contaminated by them.

4.2.5 Inadequate shielding of welds during electrode fabrication [2,5]:

Type I defects may be attributed to inadequate shielding of welds during electrode fabrication which can result in nitrogen rich weld metal. Defects may be attributed to the use of metal-inert gas (MIG) welding, if the welding process is not shielded well enough to exclude contamination. Welding of sponge electrodes with plasma torches produces a wide gradient of metallic content as the host being welded contains sponge particles, pure metallic additions, and master alloy particles. The use of chamber welding and specially shielded weld enclosures is necessary to assure absence of contaminated welds.

Visual Appearance: They are sometimes discolored with the characteristic gold color of TiN. Visual inspection of the welds after the electrode is fabricated often will reveal indications of poor shielding although this is not fool proof as over welding contaminated welds will destroy the visual evidence.

Metallurgical Characteristics: HIDs from this source may contain metallic alloying elements in the range from unalloyed titanium to that of the host alloy. It will be harder than the host alloy because of the interstitial content. Any cracking associated with the HID will come from deformation processing at either billet or forging stages. However, this type of defect may survive the melting and conversion processes without developing cracks.

Location in Ingot: This type of HID will be heavier than the liquid titanium and tend to sink to the bottom of the liquid pool. In multiple melting operations, each melt ingot will concentrate the HIDs in the bottom 1/3 of its length. Each melt will reduce the HID size depending on the pool depth, the alloy melting temperature, and the practice for electrode inversion between melts. It is a good practice to disallow welding in preparation of the final melt electrode because any HID embryo will have only one chance to dissolve.

4.2.6 VAR furnace leaks [2, 4, 5]:

Type I defects attributed to air leaks are most common in sliding seals (the ram feed through in most VAR furnace designs). This rarely occurs. Such condition is evidenced by a pressure increase in the furnace, unless a rapid increase in leak rate is also experienced. This may be dampened by high pumping capacity.

Visual Appearance: The defect will be rather large and appear as a hole in the remaining wafer after hot top which may appear much like a torch cut surface.

Metallurgical Characteristics: The defect will be harder than the matrix and have the metallic composition of the host ingot with a higher alpha content in alpha-beta alloys. The defect is unlikely to have cracks or voids except those associated with deformation processing. They will be large.

Location in Ingot: The defect will be localized near the top of the ingot produced when the leak occurred but may survive subsequent melting and wind up in the next ingot at a position depending on the electrode inversion practice used.

4.2.7 Ineffective Housekeeping [5]:

Type I defects are often attributed to splatter and other melt condenses within the furnace enclosure (furnace head and ancillary devices and chambers) which are finely divided and which oxidize (nitride) when such hot particles are exposed to air - this is generally associated with opening the furnace and exposing the virgin alloy splatter to the atmosphere. Subsequent melting may see these particles fall in the molten pool and survive by rapidly sinking to the bottom or sides - most common when the pool is shallow such as at the arc strike or in the hot top operation. This sort of defect may occur in VAR as well as CHM operations.

Metallurgical Characteristics: The origin of the source may have come from another heat of material, therefore the metallic composition could be anything. In this case the HID will be harder than the matrix, and due to the possibility of inter-alloy mixing, there may be a very different microstructure. The defect is unlikely to have voids or cracks associated except when worked. They are likely to be regularly shaped but not exclusively. They are likely to be smaller than the first 6 HIDs described above.

Location in Ingot: The defects tend to be concentrated near the top or the bottom of the final melt because of the shallow pool existing in these locations. For the deeper pool situations in steady state melting, their survival is problematic and limited to the regions near the ingot surface. With some alloys the final melt is performed entirely with a shallow pool to avoid melt segregation and, in this case, these defects may occur anywhere in the ingot. The defect is not likely to be as refractory as the other HID's and is not likely to survive multiple melting.

4.3 HIGH DENSITY INCLUSIONS [2,3,5]

High-density inclusions include refractory metals (W, Mo, Ta, and Nb) or refractory metal carbides. The main source of these defects is scrap. Carbide and tungsten particles have often been traced to machine turnings cut with

carbide tools and non-consumable welding electrodes, respectively. Refractory metals have higher melting points and densities than titanium and tend to sink to the skull at the bottom of the molten pool.
Another source of high-density inclusions is ineffective housekeeping associated with equipment repair, such as TIG welding. Without proper house cleaning, inadvertent inclusion of a Thoriated Tungsten welding electrode scrap may result.
Master alloy additions of refractory metals, such as Molybdenum, are formulated to reduce the melting point so that they will completely dissolve or melt, but there is history of these sorts of particles surviving. Recent, known, events have been attributed to use of coarse master alloy particles in formulating the ingot. The key to avoiding such occurrences is to make sure that the alloy additions are small enough particle size to assure dissolution in multiply melted material.

4.4 TYPE II DEFECTS [2,3,5]

Type II defects are also known as soft alpha segregates. These defects are found in alloys containing aluminum. Type II defects are often called High Aluminum Defects (HAD) because of the significantly higher than normal aluminum content they exhibit. Another name often used to describe this sort of defect is "chicken tracks" which reflects their appearance in billet slices.
Cause: Type II alpha defects are associated with ingot pipe and void formation. As shrinkage pipe forms in a hot titanium alloy ingot, aluminum (or any other relatively volatile alloying element at the high temperature involved) evaporates rapidly from the hottest surfaces of the void, filling it with metallic vapor which condenses on cooler surfaces of the void as the ingot cools. As a result, the interior surface of the void will be coated with aluminum and/or other volatile elements, and just below the surface, the microstructure will be slightly depleted in these elements. Subsequent forging of the ingot or intermediate mill product, in the production of billet and bar, will cause the voids to close, but the temperature and time combination is insufficient to result in serious homogenization.
Visual Appearance: Areas enriched or depleted with aluminum outline portions of the original void/pipe surface and appear as Type II segregation. The result of forging the voids closed is a rather irregularly shaped zone of aluminum rich alloy (the name of chicken tracks is descriptive here) often with an alpha lean zone immediately adjacent. They appear as light and dark etching zones, respectively, in the macrostructure of product.
Metallurgical Characteristics: The aluminum content of the defect is usually somewhat higher than that of the matrix and the vanadium content may be lower in Ti Al-V alloys. However, it is not uncommon to find an associated area which is slightly lower in aluminum content and higher in vanadium that the matrix. The defect is a form of localized alpha segregation but, unlike a Type I defects, is quite ductile with a hardness usually not much greater than that of the matrix. The segregates tend to be relatively long, thin and very irregular, and small defects do not seem to have a pronounced effect on mechanical properties of annealed alloys.
Detection: When these defects are anodized, some develop a characteristic blue color. However, areas depleted in aluminum tend to etch lighter on anodizing. These areas and have been incorrectly referred to as beta segregation. They present only a small difference in elastic properties so UT inspection is not likely to detect small Type II defects.
Prevention: Good hot topping practices that minimize the area removed during billet cropping for macroexamination. A good billet slice inspection and cropping practice will virtually eliminate these defects associated with healed pipe. However, it is possible to create them with aggressive billet conversion practice and these are difficult to detect. The best practice is to avoid their creation by process control in the mill.

4.5 INGOT POROSITY

There are two primary types of ingot porosity: gas porosity and shrinkage porosity.
Gas porosity in VAR ingots has been found to be associated with residual chloride salts in the sponge. Salts have essentially no solubility in the solid metal but form vapor bubbles in the liquid phase which have been found to account for the following defects:

- Unhealed pipe in billet
- Blisters observed in Ti-8Mn sheet
- Weld porosity
- Porosity in blended elemental powder metallurgy products

Gas porosity in Plasma Arc Melted (PAM) ingots is usually associated with entrapped inert gas used in the melting operations. Subsequent VAR ought to remove these, and PAM + VAR ingot, produced normally, will be free of gas porosity.

Shrinkage porosity can be found throughout the ingot and in the pipe section. Porosity in the pipe section results from metal shrinkage and is also associated with creation of Type II defects. They can be largely avoided by good hot topping practices. High melt rates have been found to produce more ingot porosity than slow rates (better melt degassing occurs at the slow rates and the shallower pools experience less shrinkage on freezing).
Shrinkage porosity is unlikely to survive ingot conversion practices and should not be confused with strain induced porosity created during the conversion process itself. The latter often results in "clean" porosity and is often seen during UT inspection of the billet when sophisticated means, like multi-zone inspection, are applied.

4.6 ALLOY SEGREGATION [2,5,6]

Alloy segregation can be influenced by several factors including, primarily, the alloying elements added and their amounts; solidification conditions, including temperature gradients; power interruptions or other perturbations of steady state conditions; hot topping procedure; and the homogeneity of the starting material.
Segregation is most conveniently discussed in terms of the general categories of macrosegregation and microsegregation.
Macrosegregation is generally characterized by alloying element composition differences measurable over a long range such as top to bottom, or center to outside of the ingot, or its primary converted products, such as billet. The causes for this can be lumped generally into three categories:

- inhomogeneity of starting material or electrode so that the composition of the last to melt dominates the composition of the top of the VAR ingot
- Effects of directional solidification, given homogeneous electrodes, in which the melting point suppressers will concentrate in the liquid and be richest in the last to solidify, which means that the top of the VAR ingot and the centerline will likely be rich in these elements. The opposite is true of melting point raisers.
- Vaporization and re-condensation, on crucible walls, of high vapor pressure elements, such as aluminum. As the ingot lengthens when more electrode is consumed, these elements will be entrapped in the ingot surface creating an aluminum rich zone at the ingot surface. During conversion, these are lost due to intermediate conditioning, but remelted electrodes are then inhomogeneous as the greatest amount of condensate is seen towards the end of the melt (top of the crucible) as there had been much more time for the vaporization/condensation cycle to occur. These are often avoided by proper electrode formulation compensation or electrode inversion practices and, in the last case, splash ring avoidance or remelt procedures.

Microsegregation, as distinguished from inclusions with refractory characteristics, usually results from liquid/solid partitioning during solidification much as for the macrosegregation. Its manifestation will be localized in areas where concentrations of partitioned melting point suppressers in the liquid, at the liquid-solid interface, is subjected to accelerated solidification, such as a rapid reduction in heat input. Also, where the solidification conditions favor the formation of a dendritic liquid/solid interface there is a micro partitioning of liquid formers. The interdendritic zones, being the last to solidify, will entrap extraordinarily high amounts of melting point suppressers that are mostly beta forming elements. The manifestation of this is a local area with its beta transus temperature much lower than its immediate surroundings. Near transus heat treatments will expose these areas as very lean or absent of primary alpha after a subtransus thermal exposure and are called beta flecks. The controls which can minimize the occurrence of such segregation include the avoidance of power interruptions or abrupt negative changes in power level, the maintenance of high thermal gradients in the liquid at the solid/liquid interface, and the adherence to the Tiller model for the conditions that favor the formation of planar interfaces which include, besides the establishing of high temperature gradients in the liquid, low interface velocity, and effectively removing the build up of solute in the liquid at the interface.
There are some other liquid phase formers which segregate but do not form beta flecks because subsequent solid state transformations result in discrete precipitates. The most common amongst these is silicon, which can, if large amounts are in the alloy and the proper solidification conditions are not present, result in bands of higher than normal concentration of discrete silicide precipitates. There is considerable controversy regarding the impact these bands have on properties, but there is no disagreement that there is no harm in avoiding them and this is the safe thing to do.
The beta flecks, in an alpha-beta heat treated microstructure, can reduce the fatigue properties due to microstructural discontinuities which produce elastic property discontinuities as was found in low cycle fatigue testing of Ti-5Al-2Sn-2Zr-4Cr-4Mo (Ti-17) alloy.

4.7 SYNOPSES OF EXPERIMENTAL WORK

This section contains synopses of several articles which were associated with or related to defect removal, sources of nitride inclusions, nitride seed development, and the effect of defects on fatigue properties.

4.7.1 Nitride Inclusions In Titanium Ingots: A Study Of Possible Sources In The Production Of Magnesium-Reduced Sponge (1973) (Ref. A1)

Purpose: The objective of this experiment was to demonstrate how impurities may be introduced into titanium sponge during manufacture by the magnesium reduction process and to determine under what conditions they contribute to the formation of defect-forming impurity clusters that persist through the ingot melting cycle.

Conclusions: When contaminated by an air leak during the distillation cycle or when made from air contaminated magnesium, a large variation in nitrogen content was found in the magnesium-reduced titanium sponge. TiN and Ti_2N were found in the highest-nitrogen regions. The observed nitrides were not in the form of hard, high-density particles. However, the friable pieces, powder pockets or loose powder may be compressed during electrode pressing and subsequently sintered, during melting, from the heat of the arc to produce higher-density particles. These higher density particles can survive arc melting.

Color and texture are not reliable criteria for spotting these sort of defects during sponge inspection. During both the reduction cycle and the distillation cycle, air-burned and nitrided sponge may change its color and texture. The sponge particles act as nuclei for sponge growth and may be found partially or completely clad by newly formed sponge.

It is not clear that HIDs with these physical characteristics have been unambiguously identified in any multiple melted VAR heat but the possibility for their existence still exists [5].

4.7.2 Alpha Segregation In Titanium Alloys (1980) (ref. A23)

Purpose: An experiment was conducted by creating an artificial "pipe" to show that Type II (alpha segregation) defects form in pipe cavities and is a result of non-uniform evaporation and redeposition of relatively volatile alloying elements such as aluminum.

Experiment/Conclusions: An ultrasonically sound Ti-6Al-4V square billet was heated to 1700°F and the corners were severely pressed in such a way as to deliberately create center bursts which would be detectable by UT inspection. After the billet was forged, cooled and conditioned, the piece was reheated to 2050°F for six hours and forged. Ultrasonic inspection showed no defects and slices cut from areas previously showing sonic indications showed the characteristics of Type II alpha segregation.

4.7.3 Removal Of Defects From Titanium Alloys With Electron Beam Cold Hearth Refining (1985) (ref. A2)

Purpose: An experiment was conducted to evaluate the EBCHM process for removal of defect particles from liquid titanium to prevent inclusion formation in ingots.

Experiment/Conclusions: Various materials including carbide tool chips, nitrided sponge, and flame-cut titanium scrap were used as seed in sub-scale EBCHR experiments.

All of the tungsten carbide tool bit seeds were located in the hearth skull using x-ray inspection after melting of a tungsten carbide tool bit seeded electrode which was fabricated from Ti-6Al-4V scrap. The hearth skull was then remelted several times to show the dissolution rate of HDI's to be roughly 20 microns/sec.

The flame cut scrap was drip melted and cast into ingots twice. The ingot produced contained Type I defects and was used as melt stock for EBCHM. The material was melted twice in the hearth until cast into an ingot. One defect was detected in the ingot and was attributed to a large transient in the process in which a piece of the electrode fell into the front end of the hearth at the same time that a high voltage arc extinguished the electron beams. The large flow of metal washed over the piece of electrode in the hearth and carried the defect over the lip into the ingot mold.

To understand the behavior of HID's, an experiment was run by seeding Ti-6Al-4V bars with cutting slag and nitrided sponge. Though HID's are sometimes believed to be less dense than the liquid surrounding them, their density is actually greater than the liquid and they sink. The analysis is still in progress, however, the seeds that were located were all beneath the surface of the liquid down to the solid-liquid interface. It was shown that HID's settle rapidly to the solid-liquid interface and then process to dissolve at a rate determined by the temperature at that interface.

4.7.4 Development Of Seeds For Reproducible LDI's In Titanium Melting Tests (1986) (ref. A20)

Purpose: The paper discussed the manufacture and evaluation of artificial HID formers (seeds).

Experiment/Conclusions: Sponge particles were nitrided in a furnace containing flowing nitrogen at partial pressure less than one atmosphere to produce a uniform gold color with an of average 12 to 15% nitrogen. The particles were crushed and 200 of the particles were dispersed uniformly throughout the sponge compacts and triple VAR

melted. UT inspection to a #2 FBH detected 9 HID's. Although larger, the defects exhibited a similar microstructural appearance, nitrogen content, and microhardness value to that of a natural HID.
While these seeds do help with experiments designed to understand the survivability of nitrogen stabilized sponge in the VAR process, they are clearly not realistic in that they are purely sponge source, have been crushed to irregular shapes, and probably do not contain the internal porosity generally associated with actual burned sponge. As a result, their apparent density will be higher than actual defects and the lack of internal porosity reduces their detectability. Also the nitrogen content is higher, therefore their refractory nature will be more severe than any of the actual burned sponge. Any conclusions drawn by use of such nitrided and crushed sponge will clearly indicate survivability in VAR processes much greater than expected for realistic defects but fails to address the near neutral density particle that has a greater chance of surviving a cold hearth melt by virtue of their not sinking to the skull. [5]

4.7.5 Electron Beam Melted In-Spec Titanium Remelt Electrodes (1986) (ref. A4)

Purpose: This paper discussed a recycle system to incorporate both alloy and oxygen correction during the Electron Beam (EB) melt instead of during the first Vacuum Arc Remitting (VAR) melt. Electrodes whose chemistries have been fully correct during the EB melt are called "in-spec" electrodes and require only one consumable VAR melt to meet specification requirements. EB melting, commonly called EBCHM (Electron Beam Cold Hearth Melting) is used as a method for consolidating titanium machine turnings into electrodes suitable for consumable VAR. The residence time of the large water-cooled copper hearth used in EB melting effectively removes high-density contaminants, such as carbide tool bits and refractory metals. The water cooled copper hearth of the EBCHM process affords the molten titanium additional exposure to the effects of furnace vacuum electron beam superheat and this additional residence time may help reduce or eliminate Type I defects. In a US Bureau of Mines study [ref. A15] entitled, "Type I defects: their causes and methods of elimination," skull melting was identified as a melting process capable of dissolving Type I defects.

Conclusions: The first attempts at EB melting an aggregate blend of machine turnings, sponge, 85-15 Al-V master alloy, and aluminum were less than completely successful. When the initial "in-spec" electrodes were EBCH melted, using a series of conventional master alloy particles crushed to various sizes including the standard size range, master alloy segregation occurred. To solve this segregation problem, a master alloy lot, in which the geometry of the individual particles more closely matched the geometry of the machine turning scrap, was used. By blending components selected for both size and geometrical consistency, segregation during feeding was eliminated. This indicates that to get homogeneous ingots, the master alloy cannot all sink into the skull at the early stages of melting. Increasing the surface to volume ratio of the master alloy particles, as was done, accomplishes this objective[5].

4.7.6 Melting Of Nitride Seeded Ti 6-4 Alloy Ingots (1988) (ref. A15)

Purpose: Purpose of the paper is to evaluate the capability of the ISM (Induction Slag Melting) and CVAR (Consumable Electrode Vacuum Arc Melting) processes as a method of dissolving hard alpha defects introduced by contaminated input materials. Two parallel experiments were performed. One experiment used titanium sponge manufactured in a small-scale laboratory facility while the other used commercially available sponge. Non-contaminated control ingots and contaminated ingots were made from each set of sponge material using both melting processes.

Conclusions: Alpha formers were somewhat more readily dissolved during the ISM process than during the CVAR process. This was believed to be a result of a somewhat longer residence time in the molten state and the induction stirring furnaces which may serve to buoy up nitride particles and increase their residence time in the melt as compared to the CVAR process. During CVAR melting high nitrogen areas in the consumable electrode appear to sinter to high density either in the electrode behind the arc or during melting and passage through the arc. The particles fragment during passage through the arc or in the molten pool to result in more, but smaller, defects, which are believed to be more difficult to dissolve in the molten pool due to their high sintered densities.
The ISM process will also generate a bit more superheat and a few degrees of temperature is very effective in dissolving refractory particles. Temperature is much more important than time, as the time for dissolution is related to the square root of time, while it is related to an exponential with temperature [5]. The statement regarding the concurrent sintering and fragmentation of nitrided particles during passage through the arc in a VAR process is a bit puzzling and not totally consistent with observations of nitrided sponge related HIDs [5].
Smaller seeds that have a higher surface to volume ratio also dissolve more rapidly. It is not clear that the nitrogen content, and therefore melting temperature, will be affected by any of the processes described. Therefore, fragmentation will be nothing but helpful no matter what went on before [5].

Neither induction slag or even the more scaleable induction skull process, which is based on the former, is currently scaleable to production size heats [5].

4.7.7 Utilization Of Electron Beam Melting In The Production Of Defect Free Ti-6Al-4V Ingots (1988) (ref. A3)

Purpose: The purpose of this experiment was to produce a defect-free, "in-spec EB/VAR" titanium alloy ingot.

Experiment/Conclusions: Prior to producing a "in-spec EB/VAR" ingot three experiments were conducted to evaluate the removal of dense particles during EB melting, removal of Type I defects during EB melting, and composition control of EB cast product.

During the first experiment, dense particles (tungsten to carbide tool bits) were successfully removed (excluding nitrides) from the ingot through entrapment in the hearth. The second experiment involved contaminating the input materials with infoliated billet-end crops, which have extensive oxyacetylene flame cut residual metallic drool, characteristic of surface titanium nitrides. Sonic inspection of the EB cast product to a #3 FBH defect confirmed sonic indications in only one of the three ingots that were cast. It was believed that continued efforts were required on furnace design and melt control software to provide adequate residence time and/or temperatures to guarantee Type I defect dissolution. In the third experiment, compositional control of the EB cast product, was accomplished by controlling the mixing and blending practice through the use of computer models.

A production quantity "in-spec" first stage EBCHM electrode was completed in 1985. No Type I or HDI defects were detected through sonic testing to a #2 FBH defect. The input material consisted of a large portion of scrap. The compositional variations for aluminum, vanadium and oxygen were within the range expected for a single melt process. Oxygen variability, however, was higher and attributed to a greater tendency for freezing segregation due to the sampling technique and appreciable variability in oxygen analytical techniques.

4.7.8 Standardizing Defects For Titanium Seeding Experiments (1990) (ref. A21)

Purpose: The purpose of this paper is to discuss a process which was developed to generate sponge particles with predictable nitrogen levels between zero and 15% and to establish a seeding procedure.

Experiment/results: Sponge particles were nitrided at various temperatures (1400°F-2300°F) for five minutes in a 95Ar-5N_2 atmosphere. The particles were subsequently crushed which allowed the weight and nitrogen content of both the brittle surface material and the more ductile core to be determined. The higher the temperature, the greater the nitrogen content of the particle. It was found that the bulk nitrogen content of the ductile core decreased to zero as the upper nitriding temperature (2300°F) was reached.

Many experiments have used seeding densities varying from one defect in 20 pounds to one defect in 5 pounds. Recent trials have used the higher density to affect a more stringent test. To avoid agglomeration possibilities, the following HID seed mix was recommended:

Particle Size	Amount
0.25 inch diameter Ti-15N seeds	one per five pounds
0.25 inch diameter Ti-2N seeds	one per five pounds
0.25 inch diameter Ti-8N seeds	one per five pounds
0.12 - 0.25 inch diameter production, burned sponge particles,	one particle per fifty pounds
2 inch by down torch cut sheet stock (Ti-6-2-4-2 or Ti 6-2-4-6) representing flame cut cobbles or Feed stock A	one particle per 250 pounds

The following HDI seed mix was also recommended in the interest of establishing a common standard for all seeding efforts:

Particle Size	Amount
3/8" /+ 1/4" mesh	37%
1/4" /+ 8" mesh	25%
8" /+ 14" mesh	15%
14" /+ 20" mesh	10%
20" /+ 40" mesh	8%
40" /+ 60" mesh	5%
one whole WC tool bit at midpoint of melt, 0.04" diameter Mo wire, 1/4" to 1/2" long	one particle per 125 pounds
one piece of angular Mo 1/4" diameter	one particle per 250 pounds

one piece of angular Ta 1/4" diameter	one particle per 250 pounds
one piece of 0.03" diameter W wire, (1/4" to 1/2" long)	one particle per 250 pounds
one piece of angular W 1/4" diameter	one particle per 250 pounds

4.7.9 Test Melting OF TiN and WC Seeded Ti-6-4 and Resulting Ingot Structures - A Progress Report- (1991) (ref. A22)

Purpose: The purpose of this experiment is to evaluate the advantages of EBCHR for improved cleanliness of Ti-6-4 in comparison with conventionally process VAR materials and to examine the capability of EBCHR for the production of in-specification chemistry of the Ti-6-4 alloy.

Experiment/Conclusions: Test melts of TiN and WC seeded and un-seeded Ti-6-4 were produced by EBCHR, by double VAR, and by the combination of EBCHR and VAR. The EBCHR test melts produced two unseeded and one seeded ingot, in which the seeded and one unseeded ingot were further VAR processed to produce two EBCHR-VAR ingots. One seeded ingot was produced by double VAR. The unseeded EBCHR, un-seeded EBCHR-VAR, seeded EBCHR-VAR, and seeded double VAR ingots were forged into bar. Defects were detected by x-ray in only the double VAR bars. Microscopic skull analysis of the seeded ingot melted by EBCHR showed both WC and TiN particles in the liquid-solid interface.

4.7.10 The Role Of Melt Related Defects In Fatigue Failures Of Ti-6Al-4V (ref. A17)

Purpose: The purpose of the study was to quantify the reduction of fatigue life caused by high interstitial defects (HID) and high density inclusions in titanium nitride and tungsten carbide seeded double vacuum-arc remelted titanium alloy Ti 6Al-4V.

Experiment: Two lots of material, one triple VAR and one seeded double VAR, were tested. The seeded melt contained compacts of master alloy, elemental aluminum, elemental vanadium, 5% recycled Ti 6-4 scrap, 1.8% nitrided titanium sponge (about 40 each 3 to 6 mm sized seeds/kg), and 0.079% tungsten carbide tool bit inserts (about 0.02 seeds/kg). The 16-inch diameter seeded ingot was beta forged to 8-inch diameter, and the top 1/8th of the ingot was alpha/beta forged to 3-inch diameter according to conventional practices. The 3-inch unseeded triple vacuum melted material was solution heat treated and overaged.

Conclusions: Fatigue testing of the seeded and unseeded materials showed that both high interstitial defects and high density inclusions defects can reduce fatigue life by an order of magnitude.

UT Software:

SNCALC1: A Fortran software package which allows the user to make rapid, first-order estimates of root-mean-square grain noise levels, flaw signal amplitudes, and signal-to-noise (S/N) ratios for normal-incidence, pulse/echo immersion inspections of flat or curved metal specimens. For flaw signal amplitude and S/N calculations, the defect may be either a flat circular crack (i.e., flat-bottomed hole) or a spherical inclusion. This code can be used to compare inspections which use different transducers, and to determine which transducer is likely to produce the largest S/N ratio, and hence to optimize the inspection. The code is accompanied by a 33 page user manual, "User Notes for SNCALC1: Software for Rapid Estimates of RMS noise levels and Signal-to-Noise Ratios"; Report number ISU/ETC-2. (Margetan)

UTSIMQ: Allows calculation of UT waveforms for small flaws using the Gaussian-Hermite beam model; also included are a variety of utility programs for computing system efficiency factors, doing FFT's, etc. (Gray)

FMODEL: Similar to the "utsimq" executable, except this version is greatly optimized for speed (more than an order of magnitude), but lacks some of the flexibility of "utsimq", especially regarding flaw orientation. (Gray)

MF: Software for estimating the geometrical focal length of a broad-band, spherically focused ultrasonic transducer. (Gray)

PROPOSED
TECHNICAL SPECIFICATION
FOR
PORTABLE EDDY CURRENT INSTRUMENT

funding provided by the
Federal Aviation Administration
through the
Engine Titanium Consortium

TABLE OF CONTENTS

1.0 SCOPE

This specification establishes the performance, design, development and test requirements for the Portable Eddy Current Instrument (PECI). The instrument shall have the ability to be interfaced with the Data Acquisition System, Portable Eddy Current Scanner and Shop Eddy Current Scanner* as indicated in Figure 1 and described in Section 2.0 (BACKGROUND).

2.0 BACKGROUND

The development of this specification was proposed by the Engine Titanium Consortium (ETC), a Federal Aviation Administration (FAA) sponsored program chartered to provide improved inspection capability for titanium material to be used in the manufacture of commercial jet engine components. The participants in the consortium are Iowa State University, AlliedSignal, General Electric and Pratt & Whitney. The four major tasks of the ETC program are Fundamental Studies, Probability of Detection, Ultrasonics and Eddy Current In-Service Inspection. There are nine subtasks under the Eddy Current In-Service Inspection task, one of which is the subject of this specification development.

The Portable Eddy Current Instrument subtask involves:

- review of the state of the art of commercial eddy current instrumentation
- review of advanced 'lab' capabilities
- development of this specification
- demonstration of 'some' of the advanced capabilities in an instrument developed with this specification

The technical requirements for the PECI were defined in conjunction with the other subtasks in the Eddy Current In-Service Inspection task, particularly with regards to communication and interfacing. The products of the Eddy Current In-Service Inspection task are typically referred to as 'tools' since they are available as a stand alone unit or can be integrated, as needed to meet the requirements of the inspection application. The tools which will directly interface to the PECI are the Data Acquisition System (DAS), Portable Eddy Current Scanner (PECS) and Shop Eddy Current Scanner* (SECS). Note that under the FAA program the Shop Eddy Current Scanner subtask will involve the development of a specification and no hardware will be produced. The DAS will communicate to the PECI through a high-speed digital interface for instrument parameter control and acquisition and processing of eddy current (EC) data. Both the PECS and SECS will provide for the manipulation of EC probes and will serve as an interface for the EC signals to the PECI.

This specification was developed because no single commercially available eddy current instrument is able to provide all of the eddy current inspection capabilities needed to apply recognition and processing techniques. This includes multi-frequency drive, multi-channel, array probe compatibility, remote display and high-speed digital data interface for real-time data post-processing. The purpose of this specification is to define the EC instrumentation needs of the aircraft engine industry.

3.0 DESIGN CONCEPT

Conceptually, the PECI is envisioned to resemble a ruggedly packaged version of a laptop computer and docking station with state of the art EC circuitry and high performance data acquisition, processing and display capabilities. The multi-channel eddy current interface would be used to drive multiple discrete EC elements and provide synchronization to an array probe multiplexer. The probe drive would be a constant current source with independently controllable frequency and amplitude for each EC channel. The EC channel would have a bridge and reflection element configuration capability. An interface for a remote heads-up or head-mounted display would be available with NTSC or VGA capability.

4.0 REQUIREMENTS

The requirements defined in section 4. pertain to an EC system capable supporting multiple independent EC channels. All standard element configurations will be supported which include absolute and differential/bridge and induction (reflection) types. A single EC channel is defined as having a drive output and two receive inputs.

4.1 DRIVE

The drive system shall be capable of supporting multiple independent EC channels.

4.1.1 Drive Characteristics

The probe drive shall be a variable sinusoidal current source with a maximum amplitude of 0.5 amps (peak) and adjustable in steps of 1%. For bridge type probes, software selectable internal 100 ohm resistances shall be provided for bridge drive purposes.

4.1.2 Frequency

The probe drive shall have a sine and square wave capability and operate over a frequency range of 100 Hz to 20 MHz. Three (3) simultaneous, selectable, independent frequencies shall be available per EC channel. A swept frequency capability shall be provided over a user selectable frequency range and sweep rate. The sweep range shall be up to two (2) decades over the whole operating frequency range and the rate shall be variable and dependent on the range selected. The control and communication circuitry shall be provided for a 8X multiplexer to permit array probe operation (section 4.1.4).

4.1.3 Multiple Probe/Element

Eight (8) EC channels shall be provided for multiple probe or multiple element capability. The ability to synchronize the drive signals to effectively provide a common drive which is useful for array probe operation is needed. For the common drive case, drive control shall not be independent but shall provide the other drive capabilities as described in section 4.1.1 and 4.1.2.

4.1.4 Array Probe

The capability of supporting an array probe with up to 64 elements (64 EC channels) shall be provided. Array probes with more than eight (8) elements (requiring greater than 8 EC channels) shall be accommodated through the multiplexer interface. The maximum number of elements per group is eight (8) corresponding to the eight (8) EC channels. A separate multiplexing unit shall be provided for interfacing the array

probe to the PECI through the probe interface (section 4.5.1) and multiplexer interface(section 4.5.11) as illustrated in Figure 3.

4.2 DETECTION

The detection system shall be capable of supporting multiple independent EC channels.

4.2.1 Gain

Overall gain shall be adjustable over a range of -20 dB to 100 dB independently for each EC channel. Pre-amplification (prior to demodulation) shall be adjustable over a range from -20 dB to 20 dB. Post-amplification (post demodulation) shall be adjustable from 0 to 80 dB. Both gain adjustments shall be in steps of 0.1 dB.

4.2.2 Demodulated Signal Bandwidth

The per channel EC signal bandwidth after detection shall be at least 3 kHz (-3 dB) for linear scanning and 10 kHz (-3 dB) for rotary scanning (bolthole scanning).

4.2.3 Probe Balance

Software selectable internal balance elements for absolute element balancing shall be provided with the values of 50 and 125 ohms and open circuit for external balance.

4.2.4 Sensitivity

The input sensitivity shall be a minimum of 1 kV per ohm at maximum gain setting.

4.2.5 Saturation Detection

A front-end circuitry saturation condition shall be detected and presented as both a visual indicator (to the user) and through software as a status flag.

4.2.6 Noise level

The noise level shall be held to less than half of the quantization error introduced in the digitization circuitry, which shall be approximately 0.1 mV peak.

4.2.7 Drift

Drift (output) shall be limited to 0.005 volts per hour with post-gain set at maximum (80 dB).

4.3 PROCESSING

Processing refers to the digitization and manipulation of the demodulated EC signal. Manipulation refers to the processing of digital EC data.

4.3.1 Digitization

The data sample size shall be at least 14 bits per component (in-phase and quadrature) per EC channel. The sampling rate shall be variable, externally triggerable and user selectable based on a counter with a minimum 24 bit resolution and referenced to the probe drive frequency.

4.3.2 Filtering

Filtering shall be implemented through both software and hardware providing a greater measure of flexibility and control of the filter characteristics. Low pass and high pass filter characteristics shall be provided for each component of all EC channels. Selectable filter types shall include Butterworth, Bessel and linear Phase. Filter time, frequency and delay responses shall be presented graphically for selected filter parameters. The slope of the filter cutoff characteristic shall be selectable from 1st through 6th order. A filter range shall be specified depending on the desired filter characteristics. Filter ranges of 50 Hz, 100 Hz, 200 Hz, 500 Hz, 1 kHz, 2 kHz,

5 kHz, 10 kHz (limited only by the sample rate) with a resolution of 1% for each range shall be provided. Note that all of the filter ranges may would not be required for linear scanning (section 4.2.2).

4.3.3 Frequency Domain

A post processing capability to perform a Fourier transform (DFT/FFT) shall be provided. This includes standard pre-processing features such as windowing, padding (time and frequency domain) and selectable buffer size.

4.3.4 Phase

The phase adjustment shall be from 0 to 359.9 degrees in 0.1 degree increments.

4.4 DISPLAY

The display shall have grey scale and color capability for image presentations as well as traditional views such as impedance plane and horizontal/vertical versus time. The gating for inspections should provide combined amplitude and phase windows with alarms .

4.4.1 Presentation

Real-time display shall include standard amplitude versus time and impedance plane as well as the "waterfall" (pseudo-surface) and image type. The display capability shall be a minimum of four (4) simultaneous views (i.e., 4 impedance plane or 2 impedance plane and 2 amplitude /time) of the standard display types. A single image view can be used for a real-time array probe display. 256 colors shall be provided for display of image data. The EC signal display source can be selected from the real, imaginary, magnitude or phase component. An amplitude versus frequency display can be performed in a post inspection mode. Mixing two components from separate EC channels shall be provided. The screen sensitivity shall be independently adjustable for each display and for each axis. Standard EC instrument functions such as null and erase shall be provided.

4.4.2 Alarms

Three amplitude/phase box/pie shaped gates with alarms shall be provided for each display. Combination and logical thresholding shall be provided.

4.4.3 Print Capability

A print capability shall allow a screen dump to a dot matrix printer and a post script printer. Also a screen dump can be sent to a file in one of several standard image file formats like TIFF, BMP, GIF as well as color postscript format.

4.4.4 Remote Display

An optional remote display capability shall be provided for a heads-mounted style display (see section 4.5.6). Expected cost for the head-mounted display device is less than $1K.

4.5 INTERFACE

The instrument shall have a front panel interface for a single probe connection with the capability to drive all probe types (as described previously) and a manual user interface. Several rear panel interfaces shall provide remote instrument control and set-up capabilities, EC probe and array probe connections, remote display capability and a scanner interface.

4.5.1 Probe Connection

A single EC channel shall be accessible from the front panel. All eight (8) EC channels shall be accessible on the rear panel through a high-density connector including the array probe multiplexer control signals. Power (+/- 15 volts DC @ 1.5 amps) for array probe support or a probe buffering capability shall be provided through the high-density connector.

4.5.2 Probe Adapters

Adapters shall be provided to permit the use of probes produced by various EC instrument manufacturers such as Forster, Hocking, Rohmann, Staveley, Uniwest and Zetec. The adapters shall provide an integral fit to the instrument case to support the load.

4.5.3 Remote Programmability

An RS232 industry standard serial interface shall be provided for remote setup and control of all instrument parameters. Full read and write capability shall be provided using ASCII command language structure.

4.5.4 Analog Output

Analog outputs (+/-10 volt range) shall be provided for all (8) EC channels for conventional strip chart recording or input to an alternate digitizing system. Alarms shall be generated through the analog outputs with software control of the alarm enable and threshold for each EC channel.

4.5.5 Rotating Probe

Support for speed control of a rotating scanner shall be provided with a variable DC power source (0 to +12 volts @ 2 amps). The speed control shall be accomplished through a tachometer input and supporting control circuitry under software control. A reference pulse input for display sweep synchronization shall be provided.

4.5.6 External Display

A VGA output shall be provided for connection to an external color VGA monitor or remote display. An NTSC compatible output shall be provided for remote display. The NTSC interface may not be required since head-mounted display devices are becoming available with VGA interfaces. At present, NTSC is the predominate interface.

4.5.7 Digital Parallel (interface to DAS)

DRV11J compatible

16 bit input (instrument set-up)

16 bit output (14 bit EC data, 1 reference, 1 spare) / (instrument set-up query)

4.5.8 Printer

An enhanced communication port (ECP) shall be provided as the printer interface.

4.5.9 User Input

A full keyboard interface shall be provided for the primary instrument parameter setup for functions such as null, erase, gain, frequency, etc. A smart knob shall be provided as an input device for functions, which have input options such as frequency.

4.5.10 Data Storage/Transfer

Long-term data and instrument setup storage/transfer capability shall be provided. This shall permit data and instrument setups to be saved and transferred from a

remote site without returning the instrument. This capability could be provided through the PCMCIA and SCSI interfaces

4.5.11 Multiplexer

The multiplexer interface shall provide three (3) TTL compatible lines for addressing up to eight (8) groups of elements with external trigger.

4.6 GENERAL

4.6.1 Power (power supply is not integral to unit)

Power shall be provided from an AC source or an internal battery. When operating from an AC source, a remote power converter shall provided the DC voltage to run the instrument while bypassing/recharging the battery. The power converter shall operate from 110 to 250 VAC @ 50 to 400 Hz. A lightweight battery with a 2-hour continuous operating capability shall be available as well as a longer life battery for 6 hours continuous operation.

4.6.2 Weight

Total instrument weight shall be less than 15 pounds including the short life battery (section 4.6.1).

5.0 POINT OF CONTACT

David Raulerson
Pratt & Whitney
P. O. Box 109600
West Palm Beach
FL 33410-9600
M/S 707-20
(407) 796-7683
(407) 796-7454 fax
E-mail: rauldavi@pwfl.com

BEM-Based EC Inspection Simulation Software:

A BEM-based code to allow users to perform eddy current (EC) inspection simulations has been developed by ISU as part of the novel probe design subtask of the Inservice Inspection effort. Briefly, two versions of the code, one with the field computation capability and the other with some crack modeling capability. Initially, the software task objective was to develop a code for the computer-assisted EC probe design and performance simulation. Specifically, the initial goal was to implement the field calculation capability, namely the ability to compute interrogating EC distributions on the surface of arbitrary geometry parts, induced by an EC probe of arbitrary geometry and construction. The technical approach chosen was to formulate EC processes in terms of surface integral equations and to solve them by the boundary element method (BEM). To achieve a maximum flexibility in arbitrary part and probe geometry handling capabilities, the BEM code was interfaced to a commercial CAD package (PATRAN).

The unique feature of our approach is to use the Hertz scalar and vector potentials as fundamental field variables. This method simplifies the calculations in air and ferrite core regions significantly because the Hertz vector potential vanishes identically. Although the description is less simple in conductors, the Hertz potential approach is still desirable because it describes fields correctly in the vicinity of geometrical singularities of parts, such as edges and corners. During the course of the program, the scope of the code capability was expanded to include crack signal modeling. Several factors contributed to this extended development: One is the lengthened duration of the ETC Phase I Program. Second, the supplementary funding at ISU from NIST and NSF I/U Programs was available for leverage in the crack modeling module development. Third, Chao's crack modeling effort, which he started while at ISU and continued at PW, started to yield crack signal predictions. The ISU version of the full BEM code, including crack modeling and differential-reflection probe capabilities, has been completed after the Phase-I Program ended, under the funding from NIST and NSF I/U Programs. Transfer to ETC partners will occur as applicable as part of the CNDE I/U program. (Nakagawa)

References

[i] Three volumes of the Open Forum Proceedings have been published documenting all aspects of the ETC Phase I program.

[ii] M. F. X. Gigliotti, R. S. Gilmore, and L. C. Perocchi, "Microstructure and Sound Velocity of Ti-N-O Synthetic Inclusions in Ti-6Al-4V", Metallurgical and Materials Transactions A, Vol. 25A, pp. 2321-2329 (1994).

[iii] F.J. Margetan, K.Y. Han, I. Yalda, Scot Goettsch, and R.B. Thompson, "The practical application of grain noise models in titanium billets and forgings", Rev. of Progress in QNDE, 14B, D.O. Thompson and D.E. Chimenti, eds., (Plenum Press, N.Y., 1995) p. 2129-2136.

[iv] C.P. Chiou, F.J. Margetan and R.B. Thompson, " Ultrasonic signal characterizations of flat bottom holes in titanium alloys: experiment and theory", Rev. of Progress in QNDE, 14B, D.O. Thompson and D.E. Chimenti, eds., (Plenum Press, N.Y., 1995) p. 2121-2128.

[v] I. Yalda, F.J. Margetan, K.Y. Han and R.B. Thompson, "Survey of ultrasonic grain noise characteristics in jet engine titanium", Rev. of Progress in QNDE, 15B, D.O. Thompson and D.E. Chimenti, eds., (Plenum Press, N.Y., 1996) p. 1487-1494.

[vi] F.J. Margetan, I. Yalda and R.B. Thompson, "Predicting gated-peak grain noise distributions for ultrasonic inspections of metals", Rev. of Progress in QNDE, 15B, D.O. Thompson and D.E. Chimenti, eds., (Plenum Press, N.Y., 1996) p. 1509-1516.

[vii] P. D. Panetta, F. J. Margetan, I. Yalda and R. B. Thompson, "Ultrasonic Attenuation Measurements in Jet-Engine Titanium Alloys", in Rev. of Progress in QNDE, 15B, eds. D.O. Thompson and D.E. Chimenti (Plenum, New York, 1996), p. 1525.

[viii] C.P. Chiou, F.J. Margetan and R.B. Thompson, "Modeling of ultrasonic signals from weak inclusions", Rev. of Progress in QNDE, 15A, D.O. Thompson and D.E. Chimenti, eds., (Plenum Press, N.Y., 1996) p. 49-55

[ix] F.J. Margetan, I. Yalda, R.B. Thompson, J. Umbach, U. Suh, P.J. Howard, D.C. Copley, and R. Gilmore, "Ultrasonic grain noise modeling: recent applications to engine titanium inspections", Rev. of Progress in QNDE, 16B, D.O. Thompson and D.E. Chimenti, eds., (Plenum Press, N.Y., 1997) p. 1555-1562.

[x] P. D. Panetta, F. J. Margetan, I. Yalda and R. B. Thompson, "Observation and Interpretation of Microstructurally Induced Fluctuations of Back-Surface Signals and Ultrasonic Attenuation in Titanium Alloys", Rev. of Progress in QNDE, 16B, D.O. Thompson and D.E. Chimenti, eds., (Plenum Press, N.Y., 1997), p. 1547-1554.

[xi] C.P. Chiou, F.J. Margetan, R.B. Thompson and B. Boyd, "Development of ultrasonic models for hard-alpha inclusions in titanium alloys", Rev. of Progress in QNDE, 16B, D.O. Thompson and D.E. Chimenti, eds., (Plenum Press, N.Y., 1997) p. 1529-1536

[xii] I. Yalda, P.D. Panetta, F.J. Margetan and R. B. Thompson, "Characterization of ultrasonic focused transducers using axial scans and C-scans", Rev. of Progress in QNDE, 16, D.O. Thompson and D.E. Chimenti, eds., (Plenum Press, N.Y., 1997) p. 927-934.

[xiii] F.J. Margetan, P.D. Panetta, and R.B. Thompson, "Ultrasonic signal attenuation in engine titanium alloys", in Rev. of Progress in QNDE, 17B, eds. D.O. Thompson and D.E. Chimenti, (Plenum, New York, 1998) p. 1469-1476.

[xiv] R.B. Thompson, F.J. Margetan, I. Yalda, C. P. Chiou and P.D. Panetta, and, "Coupling microstructure outputs of process models to ultrasonic inspectability ", in Rev. of Progress in QNDE, 17B, eds. D.O. Thompson and D.E. Chimenti, (Plenum, New York, 1998) p. 1847-1453.

[xv] C.P. Chiou, Isaac Yalda, F.J. Margetan, and R.B. Thompson, "The use of ultrasonic flaw and noise models in designing titanium test blocks", Rev. of Progress in QNDE, 17B, D.O. Thompson and D.E. Chimenti, eds., (Plenum Press, N.Y., 1997) p. 2069-2076.

[xvi] P. D. Panetta, R. B. Thompson and F. J. Margetan, "Use of electron backscatter diffraction in understanding texture and the mechanisms of backscattered noise generation in titanium alloys", in

Rev. of Progress in QNDE, 17A, eds. D.O. Thompson and D.E. Chimenti, (Plenum, New York, 1998) p. 89-96.

[xvii] I. Yalda, F.J. Margetan and R.B. Thompson "Use of Rician distributions to predict distributions of ultrasonic flaw signals in the presence of backscattered noise", in Rev. of Progress in QNDE, 17A, eds. D.O. Thompson and D.E. Chimenti, (Plenum, New York, 1998) p. 105-111.

[xviii] Minachi, F.J. Margetan and R.B. Thompson "Reconstruction of a piston transducer beam using multi-Gaussian beams (MGB) and its applications", in Rev. of Progress in QNDE, 17A, eds. D.O. Thompson and D.E. Chimenti, (Plenum, New York, 1998) p. 907-914.

[xix] K.Y. Han and R. B. Thompson, "Relationship Between the Two-Point Correlation of Elastic Constants and Backscattered Noise in Two-Phase Titanium Alloys", Rev. of Progress in QNDE ,Vol. 14, 67-74 (1995).

[xx] Panetta, P. D. and Thompson, R. B., "Ultrasonic Attenuation and Velocity in Duplex Titanium Alloys," Rev. of Progress in QNDE, 18, edited by D. O. Thompson and D. E. Chimenti, Plenum Press, New York, NY, in press.

[xxi] Panetta, P. D., Thompson, R. B., and Margetan, F. J., "Use of Orientation Imaging Microscopy™ in Understanding Mechanisms of Back-Scattered Noise Generation and Hard-Alpha Inclusion Reflectivity in Titanium Alloys", Rev. of Progress in QNDE, 17, edited by D. O. Thompson and D. E. Chimenti, Plenum Press, New York, NY, in press.

[xxii] Margetan, F. J., Thompson, R. B., and Lerch, T. P., "An Analytical Approximation for a Common Grain Noise Diffraction Integral," Rev. of Progress in QNDE, 18, edited by D. O. Thompson and D. E. Chimenti, Plenum Press, New York, NY, in press.

[xxiii] Thompson, R. B., "Use of UT models in titanium inspection development," Rev. of Progress in QNDE, 16B, edited by D. O. Thompson and D. E. Chimenti, pp. 1537-1545, Plenum Press, New York, NY, 1997.

[xxiv] Thompson, R. B., "A generalized model of the effects of microstructure on ultrasonic backscattering and flaw detection," Rev. of Progress in QNDE, 15B, edited by D. O. Thompson and D. E. Chimenti, pp. 1471-1477, Plenum Press, New York, NY, 1996.

[xxv] Gray, T. A.: "Application of Measurement Models to Specification of Ultrasonic Inspections," in Rev. of Progress in QNDE, 16, D.O. Thompson and D.E. Chimenti, eds., pp. 2061-2068. (Plenum Press, New York, 1997).

[xxvi] Gray, T. A.: "Ultrasonic Inspectability Models for Jet Engine Forgings," to be published in Rev. of Progress in QNDE, 17, D.O. Thompson and D. E. Chimenti, eds., pp.2053-2060. (Plenum Press, New York, 1998).

[xxvii] P. Howard, D. Copley, and R. Gilmore, "Transducer design for high sensitivity ultrasonic inspection of titanium," Rev. of Progress in QNDE, 16,A eds. D.O. Thompson and D.E. Chimenti, (Plenum Press, New York, 1997), pp.893-900.

[xxviii] J. A. Umbach, R. A. Roberts, "Ultrasonic Phased Array Transducers -Model and Experiment", presented at ASNT conference, Pittsburgh, PA, October, 1997.

[xxix] C.-P. Chiou, R. B. Thompson and L. W. Schmerr, "Model-Based Signal Processing for Ultrasonic Flaw Detection: Simulation Studies," Rev. of Progress in QNDE, D. O. Thompson and D. E. Chimenti eds., 12A, 1993, pp. 703-710.

[xxx] S. Prasad, S. Udpa, L. Udpa and C.-P. Chiou, "Detection of Hard-Alpha Regions in Titanium Using Wavelet Transform Based Techniques," Rev. of Progress in QNDE, D. O. Thompson and D. E. Chimenti eds., 13A, 1994, pp. 801-808.

[xxxi] K. Srinivasan, C.-P. Chiou, and R. B. Thompson, "Ultrasonic Flaw Detection Using Signal Matching Techniques," Rev. of Progress in QNDE, D. O. Thompson and D. E. Chimenti eds., 14A, 1995, pp. 711-718.

[xxxii] C.-P. Chiou, R. B. Thompson and L. W. Schmerr, "Ultrasonic Signal-to-Noise Enhancement Using Adaptive Filtering Techniques," Rev. of Progress in QNDE, D. O. Thompson and D. E. Chimenti eds., 14A, 1995, pp. 727-732.

[xxxiii] P. Howard, D. Copley, and R. Gilmore, "The application of a dynamic threshold to c-scan images with variable noise," *Rev. of Progress in QNDE, 17,* eds. D.O. Thompson and D.E. Chimenti, (Plenum Press, New York, 1998).

[xxxiv] P. Howard, D. Copley, J. Young, E. Nieters, and R. Gilmore, "An improved methodology for the inspection of titanium alloys," *Proceedings of the 1996 IEEE Ultrasonics Symposium, 1*, ed. M. Levy, S. Schneider, and B. McAvoy, (IEEE Press, 1996), pp. 727-730.

[xxxv] P. Howard and R. Gilmore, "Ultrasonic noise and the volume of the ultrasonic pulse," *Rev. of Progress in QNDE 15*, eds. D.O. Thompson and D.E. Chimenti, (Plenum Press, New York, 1996), pp. 1495-1502.

[xxxvi] P. Howard, R. Burkel, and R. Gilmore, "The statistical distribution of grain noise in ultrasonic C-scan images," *Rev. of Progress in QNDE 15*, eds. D.O. Thompson and D.E. Chimenti, (Plenum Press, New York, 1996), pp. 1517-1524.

[xxxvii] P. Howard, D. Copley, E. Nieters, J. Young, M. Keller, and R. Gilmore, "Ultrasonic inspection of cylindrical titanium billet," *Am. Society of Nondestructive Testing Fall Conference*, 1994.

[xxxviii] Annis, (1997) "Role of Statistical Test Design in Measuring NDE Reliability," European-American Workshop Determination of Reliability and Validation of NDE, 19 June, 1997, Berlin, Germany.

[xxxix] R.H. Burkel, D.J. Sturges, W.T. Tucker, and R.S. Gilmore, "Probability of Detection for Applied Ultrasonic Inspections," Review of Progress in QNDE, vol. 15B, eds. D.O. Thompson and D.E. Chimenti, (Plenum Press, New York, 1996), pp. 1991-1998.

[xl] Thompson, R. B., "Overview of the ETC POD Methodology," Rev. of Progress in QNDE, 18, edited by D. O. Thompson and D. E. Chimenti, Plenum Press, New York, NY, in press.

[xli] C.-P. Chiou, L. W. Schmerr and R. B. Thompson, "Ultrasonic Flaw Detection Using Neural Network Models and Statistical Analysis: Simulation Studies," Rev. of Progress in QNDE, D. O. Thompson and D. E. Chimenti eds., 12A, 1993, pp. 789-795.

[xlii] C.-P. Chiou, L. W. Schmerr and R. B. Thompson, "Statistical Detection for Ultrasonic NDE," Rev. of Progress in QNDE, D. O. Thompson and D. E. Chimenti eds., 13A, 1994, pp. 871-878.

[xliii] W. Q. Meeker, R. B. Thompson, C.-P. Chiou, S.-L. Jeng and W. T. Tucker, "Methodology for Estimating Nondestructive Evaluation Capability," Rev. of Progress in QNDE, D. O. Thompson and D. E. Chimenti eds., 15B 1996, pp. 1983-1990.

[xliv] W.Q. Meeker, S.-L. Jeng, C.-P. Chiou and R. Bruce Thompson, "Improved Methodology for Predicting POD of Detecting Synthetic Hard-Alpha Inclusions in Titanium," in Rev. of Progress in QNDE, D. O. Thompson and D. E. Chimenti eds., 16B, 1997, pp. 2021-2028.

[xlv] B. Boyd, C.-P. Chiou, R. B. Thompson and J. Oliver, "Development of Geometrical Models of Hard-Alpha Inclusions for Ultrasonic Analysis in Titanium Alloys," in Rev. of Progress in QNDE, D. O. Thompson and D. E. Chimenti eds., 17A, 1998, pp. 823-830.

[xlvi] Rough Surface Effects on Incoherent Scattering from Random Volumetric Scatterers: Approximate Analytic Series Solution, M. Bilgen and J. H. Rose, J. Am. Acoust. Soc. **96**, 2856 (1994).

[xlvii] Acoustic double-reflection and transmission at a rough water-solid interface, J. H. Rose, M. Bilgen and P. B. Nagy, J. Acoust. Soc. Am. **95**, 3242 (1994).

[xlviii] Focused ultrasonic probes and the effects of surface roughness on material noise, M. Bilgen and J. H. Rose, Rev. of Progress in QNDE, **13**, 1769 (1994).

[xlix] Doubly coherent transmission at rough surfaces and its implications for ultrasonic inspection, J.H. Rose, Rev. of Progress in QNDE, **13**, 1753 (1994).

[l] "Mean and Variance of the Ultrasonic Signal from a Scatterer Beneath a Rough Surface: Theory", M. Bilgen and J. H. Rose, J. Acoust. Soc. Am. **98**, 2217 (1995).

[li] Ultrasonic signals from "worst-case" hard-alpha inclusions beneath a random rough surface, J.H. Rose, Rev. of Progress in QNDE, **14**, 1837 (1995).

[lii] Excess scattering induced loss at a rough surface due to partially coherent double reflection, J.H. Rose, Rev. of Progress in QNDE, **14**, 1845 (1995).

[liii] Variance of the ultrasonic signal from a defect beneath a rough surface, J.H. Rose, Rev. of Progress in QNDE, **15**, 1463 (1996).

[liv] Acoustic Backscatter from materials with rough surfaces and finite microstructures: Theory, M. Bilgen and J.H. Rose, J. Acoust. Soc. Am, **101**, 264 (1997).

[lv] Acoustic signal-to-noise ratio for flaws beneath a randomly rough surfaces and in the presence of microstructure, M. Bilgen and J.H. Rose, J. Acoust. Soc. Am, **101**, 272 (1997).

[lvi] K. Smith, "Engine Perspectives on Aging Aircraft", presentation at the 41st International Symposium of SAMPE, March 1997.

[lvii] M. Gehlin, "Commercialization of the Eddy Current Scanner", Proceedings of the Open Forum, November 1997.

[lviii] M. Phalin, "Automated Eddy Current Inspection of Propeller Repairs", presentation at ATA NDT Forum, September 1996.

[lix] D. Arms, "Application of Eddy Current Inspection at United Airlines", presentation at ATA NDT Forum, September 1997.

[lx] C. Mobley, "Evaluating the ETC Portable Scanner System", Proceedings of the Open Forum, November 1997.

[lxi] A. D'Orvilliers, and D. Bryson, "Application of the ETC Portable Scanner to Disk Inspection", Proceedings of the Open Forum, November 1997.

[lxii] R. J. Filkins, J. P. Fulton, T. C. Patton, and J. D. Young, "Recent advances and implementations of flexible circuit eddy current technology", Rev. of Progress in QNDE, v. 16, ed. by D. O. Thompson and D.E. Chimenti, Plenum Press, New York, NY, 1997.

[lxiii] T. Patton, R. Filkins, J. Fulton, K. Hedengren, J. Young, C. Granger, and T. Hewton, "Development of a hand-held, flexible eddy current probe for inspection of curving surfaces", Rev. of Progress in QNDE, v. 15, ed. by D. O. Thompson and D. E. Chimenti, Plenum Press, New York, NY, 1996.

[lxiv] J. P. Fulton, K. Hedengren, J. Young, T. Patton, R. Filkins, "Optimizing the design of flexible multilayer eddy current probes - A theoretical and experimental study", Rev. of Progress in QNDE, v. 15, ed. by D. O. Thompson and D. E. Chimenti, Plenum Press, New York, NY, 1996.

[lxv] K. Hedengren, J. Fulton, J. Young, T. Patton, R. Filkins and R. Hewes, "Progress in flexible eddy current array technology", Rev. of Progress in QNDE, v. 15, ed. by D. O. Thompson and D. E. Chimenti, Plenum Press, New York, NY, 1996.

[lxvi] R. J. Filkins, J. P. Fulton, T. C. Patton, and J. D. Young, "Recent advances and implementations of flexible circuit eddy current technology", Rev. of Progress in QNDE, v. 16, ed. by D. O. Thompson and D.E. Chimenti, Plenum Press, New York, NY, 1997.

[lxvii] T. Patton, R. Filkins, J. Fulton, K. Hedengren, J. Young, C. Granger, and T. Hewton, "Development of a hand-held, flexible eddy current probe for inspection of curving surfaces", Rev. of Progress in QNDE, v. 15, ed. by D. O. Thompson and D. E. Chimenti, Plenum Press, New York, NY, 1996.

[lxviii] J. P. Fulton, K. Hedengren, J. Young, T. Patton, R. Filkins, "Optimizing the design of flexible multilayer eddy current probes - A theoretical and experimental study", Rev. of Progress in QNDE, v. 15, ed. by D. O. Thompson and D. E. Chimenti, Plenum Press, New York, NY, 1996.

[lxix] K. Hedengren, J. Fulton, J. Young, T. Patton, R. Filkins and R. Hewes, "Progress in flexible eddy current array technology", Rev. of Progress in QNDE, v. 15, ed. by D. O. Thompson and D. E. Chimenti, Plenum Press, New York, NY, 1996.

[lxx] Jay M. Amos, Joseph C. Chao, 'Optimization of a Wide-Field Eddy Current Probe using a Boundary Element Method based Model', Rev. of Progress in QNDE, p. 275, Vol 17, 7/97.

[lxxi] Jay M. Amos, Joseph C. Chao, 'Assessment of Eddy Current Inspection Development through Numerical Simulation', American Society of Nondestructive Testing Fall Conference, 10/97.

[lxxii] J.M. Amos, D.A. Raulerson, J.C. Chao, N. Nakagawa, 'Model-based Eddy Current Probe Optimization & Processing Methods for Engine Inspections', ATA Open Forum, 11/97

[lxxiii] N. Nakagawa, J. Chao, and A.N.S. Prasad, "In-service eddy current inspection and computer simulation," in *Nondestructive Testing of Materials*, eds. R. Collins, W.D. Dover, J.R. Bowler, and K. Miya, IOS Press, Amsterdam, 1995.

[lxxiv] J. C. Chao, N. Nakagawa, D. Raulerson, and J. C. Moulder, "Boundary element method based probe design model validation," in Rev. of Progress in QNDE, 16, pp. 967-972, eds. D. O. Thompson and D. E. Chimenti, Plenum Press, New York, 1997..

[lxxv] L. Brasche & K. Smith, "Engine Titanium Consortium: Status of the Contaminated Billet Study", Materials and Process Affordability Keys to the Future, SAMPE 43, p. 1458, June 1998.